

An Algorithm for the Separation-Preserving Transition of Clusterings

Steffen Borgwardt*

Felix Happach[†]

Stetson Zirkelbach*

Abstract

The separability of clusters is one of the most desired properties in clustering. There is a wide range of settings in which different clusterings of the same data set appear. A common application lies in the need for a transition of one separable clustering into another one. This transition should be a sequence of simple, natural steps that upholds separability of the clusters throughout.

In this paper, we design an algorithm for such a transition. We exploit the intimate connection of separability and linear programming over bounded-shape partition and transportation polytopes: separable clusterings lie on the boundary of partition polytopes, form a subset of the vertices of the corresponding transportation polytopes, and circuits of both polytopes are readily interpreted as sequential or cyclical exchanges of items between clusters. This allows for a natural approach to achieve the desired transition through a combination of two walks: an edge walk between two so-called radial clusterings in a transportation polytope, computed through an adaptation of classical tools of sensitivity analysis and parametric programming; and a walk from a separable clustering to a corresponding radial clustering, computed through a tailored, iterative routine updating cluster sizes and re-optimizing the cluster assignment of items.

Keywords: separability; clustering; transition of clusterings; partition polytopes; linear programming; polyhedral theory

MSC2020: 90C90, 90C05, 90C31, 62H30, 51M20

1 Introduction

1.1 Separable Clusterings

The *partitioning* or *clustering* of a data set X into a set $C = (C_1, \dots, C_k)$ of disjoint clusters is the arguably most important task in unsupervised learning. In today's world of unprecedented data collection, it arises in applications in a wide range of fields, including operations research, machine learning, and statistics.

Based on a measure of similarity of items in the data set, the goal of clustering is to assign items that are similar to each other to the same cluster. Most clustering tasks are performed in a geometric setting: the data set $X = \{x_1, \dots, x_n\} \subseteq \mathbb{R}^d$ is represented as a finite collection of

*Department of Mathematical and Statistical Sciences, University of Colorado Denver, CO, USA. Emails: {steffen.borgwardt, stetson.zirkelbach}@ucdenver.edu

[†]Department of Mathematics and School of Management, Technische Universität München, Germany. Email: felix.happach@tum.de

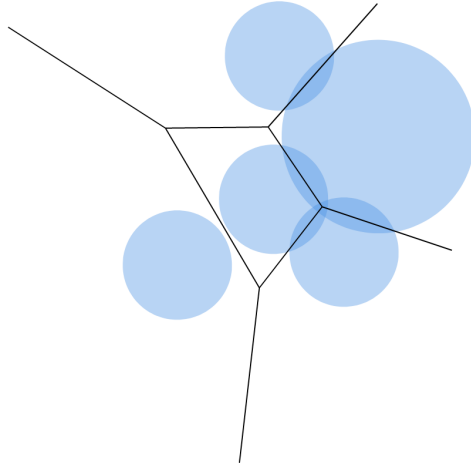


Figure 1: A power diagram in \mathbb{R}^2 . Each cell specifies a site and radius of a ball around it. Separating hyperplanes between cells run through the common intersection points of a joint scaling of the corresponding balls.

items in a d -dimensional real space, and measures of similarity correspond to a norm or quasi-norm in the space; the Euclidean-norm or squared Euclidean norm are most common. More sophisticated similarity measures are typically implemented indirectly, through the application of a kernel function to transition the space \mathbb{R}^d underlying X to a different one in which the Euclidean norm or its square again are viable to measure similarity [16].

In this setting, the desire to create clusters of similar items becomes a desire to partition the data set into *separable* clusters. Two clusters C_1, C_2 are separable if there exists a separating hyperplane between them. For clusterings $C = (C_1, \dots, C_k)$ of more than two clusters, the condition of *separability* becomes stronger: not only is separability of each pair of clusters required, but the separating hyperplanes have to *partition* the underlying space into a cell complex $P = (P_1, \dots, P_k)$ of (convex) polyhedral cells, one cell P_i for each cluster C_i . We provide formal definitions of these terms, and the terms below, in Section 2.

We call such a cell complex a *separating power diagram* for C . Power diagrams are a classical topic in computational geometry, and generalize the well-known Voronoi diagrams [1]. A power diagram can be specified through the definition of a ball, with (center-)site s_i and radius r_i , for each cell P_i . The hyperplanes separating pairs of cells are equally far from the sites with respect to a distance measure based on the corresponding balls. Geometrically, they run through the common intersection points of (a joint scaling of) the balls. See Figure 1 for an example of this construction, and Figure 2 for an example for a separating power diagram. The same concept of cluster separation appears under many other names in the literature, such as multiclass support vector machines [11, 13, 18, 19], piecewise-linear separability [4], or full site-induced cell decompositions [5].

There is a one-to-many correspondence between clusterings that ‘allow’ separating power diagrams (we will call them *constrained least-squares assignments*), and power diagrams that ‘induce’ the clustering by assigning all points in a cell to the same cluster [2]. Most importantly, a constrained least-squares assignment and corresponding separating power diagram can be constructed from the *same* sites s_1, \dots, s_k .

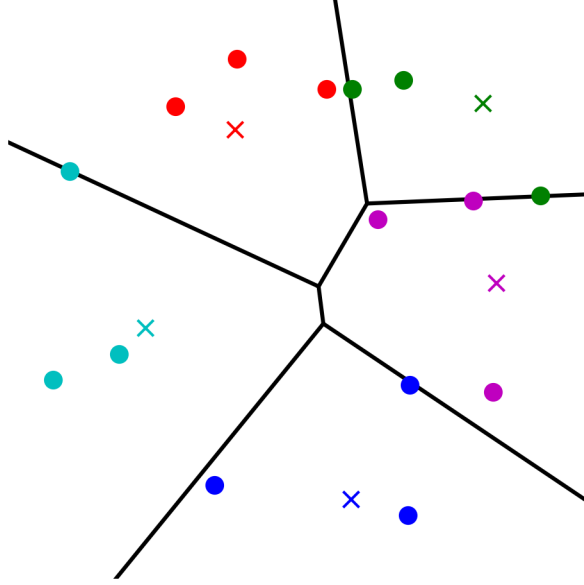


Figure 2: A separating power diagram for a clustering of five clusters (different colors) in \mathbb{R}^2 . Items of the clusters are shown as filled circles, the sites for the cells are shown as crosses (in this figure, and subsequent figures throughout the paper).

1.2 Transitions between Separable Clusterings

Our goal is to design algorithms for the transition between two separable clusterings of the same data set; we call them *initial* clustering and *target* clustering. Figure 3 shows an example. The transition should be a sequence of clusterings, each of them retaining separability, that gradually transitions the initial clustering into the target one through a series of clusterings that during the algorithm described are called the *current* clustering.

Our interest in such transitions is based on a wealth of applications in which different (separable) clusterings of the same data set appear [10]: For example, different algorithms for the same clustering task generally return different clusterings, and one may look for a formal measure for their difference that takes into account the underlying geometric structure. In other applications, there are clusterings of the same data set for different time instances, and one wants to create a model that explains how they changed over time. Such a transition would give the ability to extrapolate to possible future changes.

However, the most important driver for our work is a common situation in operations research: there is an (original) initial clustering of a data set reflecting the current state, as well as a (new, desired) target clustering that should be implemented in practice. The two clusterings may differ significantly, and one wants to devise an efficient, gradual transition over time from the initial to the target clustering.

For example, a challenge in commercial large-scale computing is the assignment of resources in a computing-cluster (a group of interconnected computers) to different processes over time. The resources in a computing-cluster are typically represented as items in a data set in a two- or three-dimensional space, with distances corresponding to the communication times between the physical elements. For efficiency, the resources assigned to the same process should be close to each other, which leads to the desire of a separable clustering of the resources.

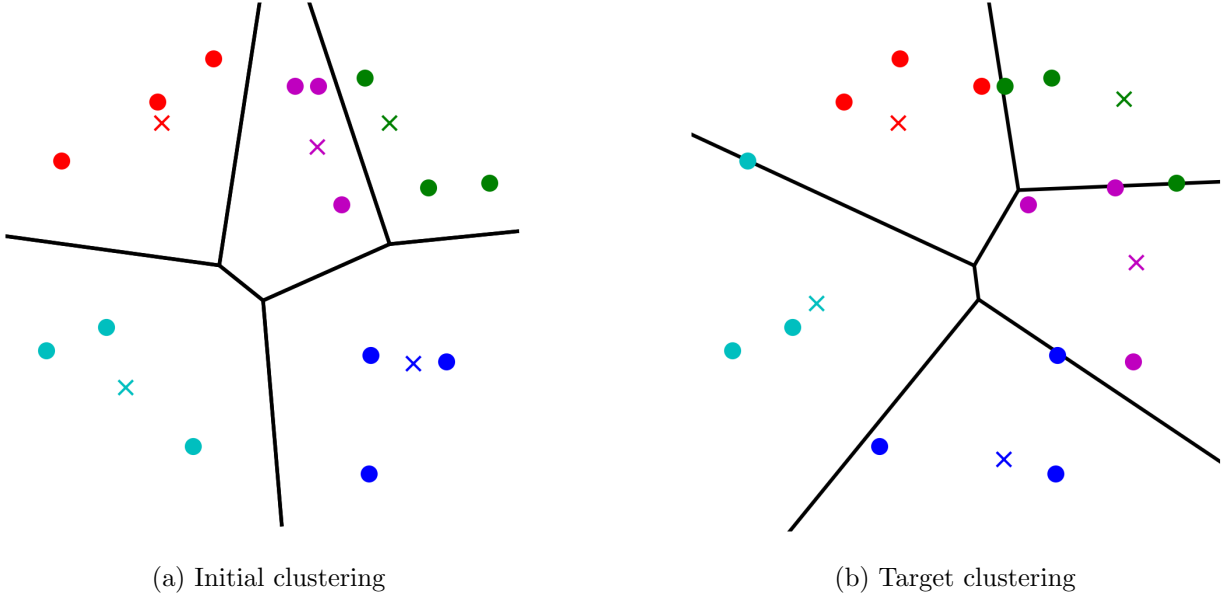


Figure 3: An initial clustering and a target clustering of the same data set. Our goal is the design of an algorithm to find a sequence of separable clusterings that gradually transitions the initial clustering into the target clustering.

The processes request different amounts of resources at different times - freeing unneeded resources or requesting more for a speed-up while they are running. Further, they finish at different times, and new processes may be started at any time. This generates the need to shift resources between processes; the planned allocation of resources changes constantly. In turn, the planned separable clustering changes constantly. At any time, there is a current separable clustering and a desired new clustering, and one is interested in a quick, gradual transition that keeps separability of the clusters, to not disrupt current processes and to keep an efficient use of resources at all times.

Further, there are many examples of such situations in the clustering of customers in service, entertainment, and insurance industry, where a company may want to transition their customers to a new clustering of premium classes over time. Upholding separability of the clusterings throughout is a key aspect to fairness of the transition.

1.3 Contributions and Outline

In this paper, we provide the theory and establish an algorithmic framework for a gradual transition between two separable clusterings, ready to be applied in practice and tailored to specific applications in future work. A key goal in the design of this gradual transition is for it to be as ‘natural’ as possible. This drives the design of our algorithms in two ways.

First, the sites used for the construction of both least-squares assignments and separating power diagrams will take a central role. Let $s = (s_1, \dots, s_k)$ be the sites for the initial clustering C^s in the transition, and let $t = (t_1, \dots, t_k)$ be the sites for the target clustering C^t . We are going to construct a sequence of clusterings that follows a *linear transition* from s to t : essentially, we want to identify the intermediate clusterings and power diagrams that occur if we linearly move the location of the sites s_1, \dots, s_k of C^s to the sites t_1, \dots, t_k of C^t . Each of these clusterings will itself be a constrained least-squares assignment for a site vector $(1 - \lambda)s + \lambda t$ for some $0 < \lambda < 1$.

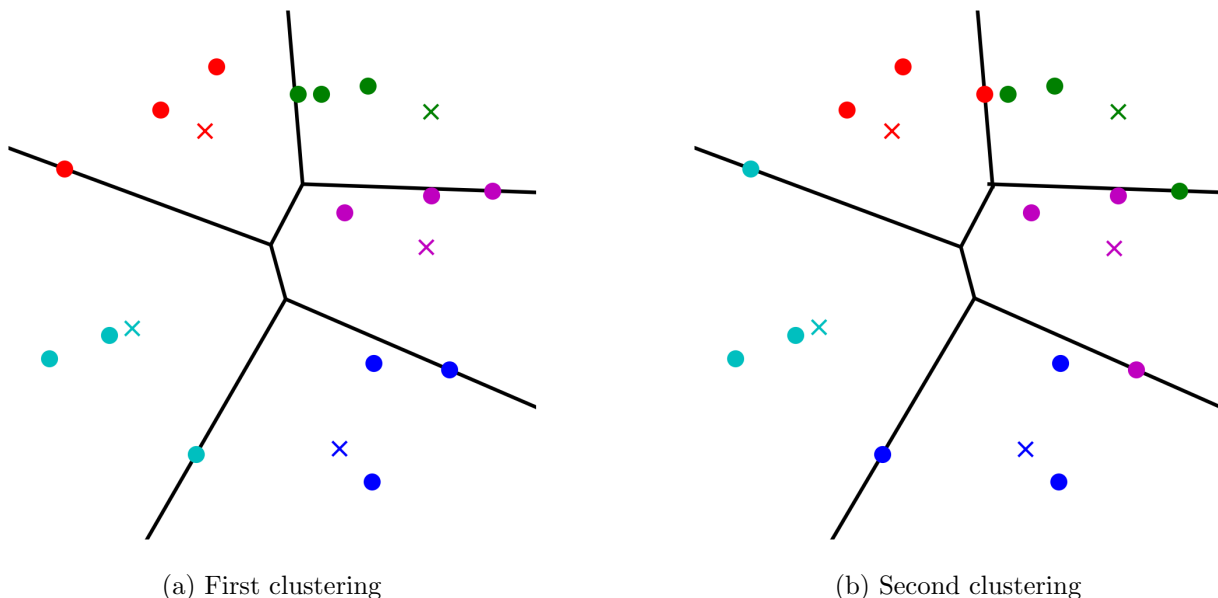


Figure 4: Two clusterings that allow a shared separating power diagram. The clusterings only differ by items that lie on the separating hyperplanes between clusters. In fact, the clusterings differ by a single exchange of such items.

Second, the transition should be a sequence of simple transitions. We are going to achieve this through the application of a so-called *sequential* or *cyclical exchange* of items in each step. For such an exchange, one selects an ordered list of clusters and one item from each cluster; the next clustering in the transition is then derived by moving the items to new clusters following the ordered list. These exchanges are a simple choice that allows for the construction of the desired transition, and they have been important in the construction of clustering transitions in easier settings and the studies of combinatorial diameters [6, 10].

Linear programming and polyhedral theory provide several powerful tools to achieve both of these goals. Separable clusterings are in one-to-one correspondence to vertices of so-called *fixed-shape partition polytopes*, and all vertices (and possibly some other boundary points) of the so-called *bounded-shape partition polytopes* \mathcal{P}^\pm correspond to separable clusterings [3, 5, 8]. Further, the set of circuits or elementary vectors of these polytopes corresponds to the desired sequential and cyclical exchanges of items [10]. This implies that, under mild assumptions, two neighboring vertices of a bounded-shape partition polytope correspond to two separable clusterings that differ by just a single exchange of this type. Further, for any two separable clusterings that lie in the same face of \mathcal{P}^\pm , there exists a site vector for which the clusterings are equally good constrained least-squares assignments. Equivalently, the clusterings allow the construction of what we will call a *shared power diagram*, i.e., a separating power diagram that induces both clusterings, with respect to these sites. Figure 4 shows an example; the two clusterings only differ by a single exchange of items that lie precisely on the separating hyperplanes specified by a shared power diagram. Finally, for a given site vector \bar{s} there always exists a constrained least-squares assignment that corresponds to an optimal boundary point of \mathcal{P}^\pm in direction of \bar{s} [5, 8, 12] – we will call these *radial clusterings* w.r.t. \bar{s} .

Together, these observations lead to an elegant approach to the construction of a transition between two radial clusterings. Due to the close connection of power diagrams and linear pro-

gramming over partition polytopes, the linear transition $((1 - \lambda)s + \lambda t$ for increasing λ) from sites s to sites t is related to sensitivity analysis and parametric linear programming, see e.g. [17]. In a simple form of sensitivity analysis, one is interested in when and how an optimal solution of a linear program changes when altering the objective function vector slightly. The ‘breakpoint’ when an optimal basis changes can be expressed via information in the corresponding simplex tableau. An adaptation of these tools will lead to an algorithm to identify *when* (for which values of λ) and *how* (which items in the data set are moved) clusterings change throughout the transition. Geometrically, we construct a walk along the boundary of \mathcal{P}^\pm .

Note, however, that not all least-squares assignments are radial clusterings; in other words, not all least-squares assignments are on the boundary of a bounded-shape partition polytope at hand. Therefore, we design a second algorithm that transitions a general constrained least-squares assignment to a corresponding radial clustering with respect to the same sites s . We call this a *fixed-size transition*. As in the previous algorithm, each step of this transition will be the application of a single exchange of items in the data set. Each intermediate clustering is a constrained least-squares assignment for the sites s ; only the number of items in the clusters changes.

A combination of these two algorithms allows for the computation of a transition of any constrained least-squares assignment into any other through a sequence of cyclical and sequential exchanges of items, while retaining separable clusterings throughout. As we will see, there are significant challenges in the implementation of this scheme. Most importantly, partition polytopes \mathcal{P}^\pm are defined as the convex hull of a set of vertices (that are not even known apriori), and there is no explicit description through a system of linear constraints. However, partition polytopes are known to be linear projections of so-called *bounded-shape transportation polytopes* \mathcal{T}^\pm , for which such a representation is available. All clusterings (not only separable ones) correspond to vertices of \mathcal{T}^\pm , and we are able to perform our algebraic computations - in particular a tailored sensitivity analysis - over these polytopes. As a favorable byproduct, we are able to specify and respect bounds on the sizes of clusters, i.e., the number of items in the clusters, for all clusterings throughout. Bounds on cluster sizes arise in a variety of situations. For example, they may be imposed directly by an application, or clustering algorithms may enforce such bounds to return clusters of similar sizes. For our purposes, we choose the size $|C_i|$ of cluster C_i to always lie between the lower and upper bounds given by the initial and target clustering, i.e., $\min\{|C_i^s|, |C_i^t|\} \leq |C_i| \leq \max\{|C_i^s|, |C_i^t|\}$.

In Section 2, we turn to some preliminaries and recall the necessary literature. In Section 3 we provide a high-level overview of our strategy. In Sections 4 and 5 we provide the necessary technical details and proofs. Section 4 is dedicated to the fixed-site transition of a general constrained least-squares assignment to a corresponding radial clustering. In Section 5, we adapt classical sensitivity analysis techniques to our purposes for a linear transition between radial clusterings. We conclude with a brief outlook on some open questions and natural next steps in this direction of research, in Section 6.

2 Preliminaries

We start with some general notation. We denote the Euclidean norm of a vector $x \in \mathbb{R}^d$ by $\|x\|$. Recall that a set $X \subseteq \mathbb{R}^d$ is called *convex* if $(1 - \lambda)x + \lambda y \in X$ for all $x, y \in X$ and $\lambda \in [0, 1]$. The *convex hull* of a set X is the set of all convex combination of X and is denoted by

$$\text{conv}(X) := \left\{ \sum_{q=1}^n \lambda_q x_q \mid x_1, \dots, x_n \in X, \lambda_1, \dots, \lambda_n \geq 0, \sum_{q=1}^n \lambda_q = 1 \right\}.$$

2.1 Clusterings, Least-Squares Assignments, and Power Diagrams

Let $n, d, k \in \mathbb{N}$ be positive integers, and let $[m] := \{1, \dots, m\}$ for $m \in \mathbb{N}$. Let $X = \{x_1, \dots, x_n\} \subseteq \mathbb{R}^d$ be a set of n distinct items (i.e., $x_i \neq x_j$ for $i \neq j$), and assume, w.l.o.g., that $\sum_{j=1}^n x_j = 0$.

2.1.1 Clusterings and Cluster Size Bounds

Definition 1 (Clustering). A clustering of X is a partition $C = (C_1, \dots, C_k)$ of X . For $i \in [k]$, we call C_i the i -th cluster and $|C_i|$ denotes its size, i.e., the number of items in C_i . The shape of C is $|C| := (|C_1|, \dots, |C_k|)$.

For the desired transition from one clustering to another, we impose cluster size bounds prescribed by the initial clustering C^s and target clustering C^t : in all intermediate clusterings in the transition, the size of the i -th cluster has to lie between the sizes of the i -th clusters in C^s and C^t . Formally, we aim to satisfy $\min\{|C_i^s|, |C_i^t|\} \leq |C_i| \leq \max\{|C_i^s|, |C_i^t|\}$ throughout.

More generally, for every $i \in [k]$, we are given a lower and upper bound on the size of the i -th cluster, which we denote by κ_i^- and κ_i^+ , respectively. Further, we set $\kappa^- = (\kappa_1^-, \dots, \kappa_k^-) \in \mathbb{N}^k$ and $\kappa^+ = (\kappa_1^+, \dots, \kappa_k^+) \in \mathbb{N}^k$. A clustering C , and its associated shape, are called *feasible* if $\kappa_i^- \leq |C_i| \leq \kappa_i^+$ for all $i \in [k]$. In the remainder of this paper, we will only consider feasible clusterings.

2.1.2 Separable Clusterings, Least-Squares Assignments, and Power Diagrams

In this paper, we study transitions between separable clusterings. Two clusters are called separable if there exists a (separating) hyperplane that partitions the underlying space into two halfspaces, each of which containing one of the clusters. A *separable clustering* $C = (C_1, \dots, C_k)$ requires separability of all pairs of clusters, as well as a special positioning of the corresponding hyperplanes: they have to create a partition of the underlying space into a cell complex $P = (P_1, \dots, P_k)$ of polyhedral cells, one cell P_i for each cluster C_i formed through the intersection of all halfspaces that contain C_i .

Separable clusterings have a representation as so-called (constrained) least-squares assignments, as we will explain below.

Definition 2 (Least-Squares Assignment). A least-squares assignment, or *LSA*, for a given site vector $s_1, \dots, s_k \in \mathbb{R}^d$ is a clustering $C = (C_1, \dots, C_k)$ that minimizes

$$\sum_{i=1}^k \sum_{x \in C_i} \|x - s_i\|^2.$$

A clustering that minimizes this term over all clusterings with the same shape as C is called a constrained (or balanced) LSA.

Most LSAs considered in this paper are constrained LSAs. We will sometimes simply call them LSAs, when the context is clear. Constrained LSAs are intimately connected to the so-called *power diagrams*. Let $s_1, \dots, s_k \in \mathbb{R}^d$. The sites $\{s_1, \dots, s_k\}$ defines a polyhedral decomposition of \mathbb{R}^d , a so-called *power diagram* [1, 2], and s is called its *site vector*. The i -th cell of this decomposition is

$$P_i := \{x \in \mathbb{R}^d \mid (s_\ell - s_i)^T x \leq \gamma_\ell - \gamma_i \text{ for all } \ell \in [k] \setminus \{i\}\}, \quad (1)$$

where $\gamma_1, \dots, \gamma_k \in \mathbb{R}$ correspond to the dual solution of a specific LP that only depends on X and s ; see [3] for more details.

Aurenhammer et al. [2] proved the following connection between power diagrams and constrained LSAs: if a power diagram satisfies $C_i \subseteq P_i$ for all $i \in [k]$, then C is a constrained LSA to the site vector s of the power diagram. We call a power diagram that satisfies this property a *separating power diagram* for the underlying LSA. Conversely, if C is a constrained LSA to a given site vector s , then there exists a power diagram with site vector s that *induces* C by assigning all items in the same cell to the same cluster (and for items on the boundary between cells to any of these cells' clusters).

Figures 2, 3, and 4 from the introduction visualized constrained LSAs and corresponding separating power diagrams. Note that both can be constructed from the same sites (marked as crosses in the figures). It is well-known that all (simple) polyhedral cell complexes (in dimension 3 or higher) can be represented as a power diagram, and thus all separable clusterings (in dimension 3 or higher) have a representation as a constrained LSA. When a power diagram serves as a separating power diagram for two separable clusterings, respectively constrained LSAs, it is called a *shared (separating) power diagram* for the clusterings; recall Figure 4.

The connection between power diagrams and constrained LSAs becomes more intuitive when using an alternative, equivalent characterization of power diagrams, see [1, 7]:

Definition 3 (Power Diagram). *For a given weight vector $w = (w_1, \dots, w_k) \in \mathbb{R}^k$ and sites $s_1, \dots, s_k \in \mathbb{R}^d$, the set*

$$P_i := \{x \in \mathbb{R}^d \mid \|x - s_i\|^2 - w_i \leq \|x - s_\ell\|^2 - w_\ell \text{ for all } \ell \in [k] \setminus \{i\}\} \quad (2)$$

is the i -th cell of the power diagram (P_1, \dots, P_k) of \mathbb{R}^d .

Figure 1 from the introduction depicts a power diagram constructed following Definition 3. It is not hard to see that the sets in (1) and (2) coincide for $\gamma_i = \frac{1}{2} (\|s_i\|^2 - w_i)$ for all $i \in [k]$. Thus, the cells P_1, \dots, P_k defined in (2) induce the same power diagram as those defined in (1). Note that we can, w.l.o.g., assume $w_1 = 0$ in (2). In this paper, we will use both characterizations, (1) and (2), of power diagrams.

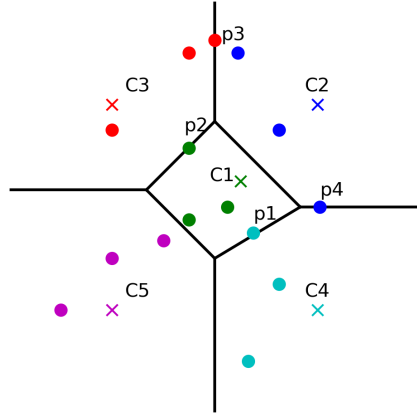
2.1.3 Clustering Difference Graphs and Exchanges of Items

To compare two clusterings in view of their difference in item assignments, we will make use of a so-called *clustering difference graph* [6]. For two clusterings C, C' , the clustering difference graph $CDG(C, C')$ is a labeled directed multigraph with one node for every $i \in [k]$ and an arc (i, ℓ) for distinct $i, \ell \in [k]$ with label x if $x \in C_i \cap C'_\ell$.

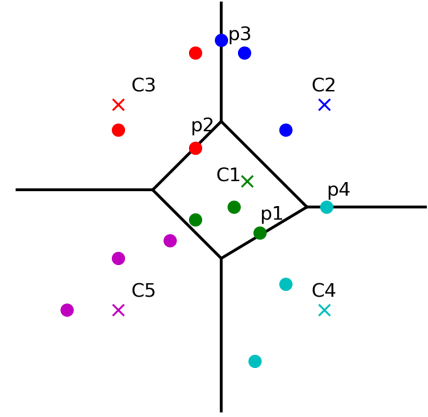
Definition 4 (Clustering Difference Graph). *The clustering difference graph (CDG) of two clusterings C, C' of X is defined as $CDG(C, C') = ([k], E)$ with $E = \{(i, \ell, x) \mid i, \ell \in [k], i \neq \ell, x \in C_i \cap C'_\ell\}$.*

For our purposes, CDGs will appear when we compare a current clustering C to a target clustering C' . The $CDG(C, C')$ is a convenient way to represent the necessary changes in the assignment of items to clusters. Informally, a CDG contains an arc from node i to node j with label x , if the item x has to move from cluster C_i to cluster C'_j (as part of any transition from C to C'). W.l.o.g., we may remove isolated nodes in a CDG; these nodes correspond to clusters that have the same items in both C and C' .

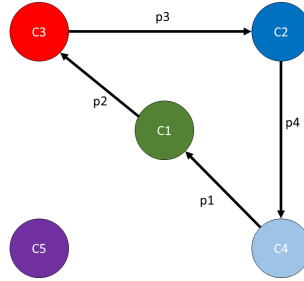
We call a cycle in a CDG a *cyclical exchange* of items between clusters, and a path in the clustering graph a *sequential exchange*. If $CDG(C, C')$ consists of a single cyclical or sequential



(a) Initial clustering and associated power diagram



(b) Target clustering that allows the same, shared power diagram



(c) A sketch of the cyclical exchange required to transition the initial into the target clustering.

Figure 5: Two clusterings (top) that allow for a shared power diagram. The two clusterings differ only by a single cyclical exchange (bot): the CDG shows clusters as nodes; the arcs between them are labeled with the items that have to be moved.

exchange, we will say that C and C' *differ* by a single exchange. *Applying* a cyclical or sequential exchange refers to updating C to the clustering C' that differs from C by only this exchange. Informally, the item reassignments indicated by the arcs of the cyclical or sequential exchange are performed. Figure 5 depicts an example.

For a transition between two clusterings, we are going to create a sequence of intermediate clusterings that differ from the next by just a single exchange. There are several arguments why this is a natural choice: the only conceptually simpler difference between two clusterings takes the form of an exchange of a single *item*. However, such simpler exchanges would immediately violate cluster size bounds if the shapes of C and C' coincide - in this case, $CDG(C, C')$ decomposes into arc-disjoint cycles, and only cyclical exchanges may be applied to retain feasible clusterings [6]. Further, our more general exchanges, in a sense, aggregate several single-item exchanges, and perform them together. This is beneficial for keeping the number of steps, respectively the number of clusterings, in the transition low.

2.2 Bounded-Shape Partition Polytopes and Transportation Polytopes

Exchanges and CDGs already have proven to be a powerful tool for the construction of clustering transitions [6, 10]. However, CDGs contain no information on the location of items in the underlying space, and thus no information on separation. This is our main goal - we aim for a transition that upholds separability of the clusters throughout. To this end, we will make use of special classes of polytopes that contain valuable information on both cyclical and sequential exchanges and separability of clusterings.

2.2.1 Bounded-Shape Polytopes and their Vertices

For a clustering C and $i \in [k]$ and $j \in [n]$, one can introduce binary variables y_{ij} that indicate whether $x_j \in C_i$ ($y_{ij} = 1$) or not ($y_{ij} = 0$). The set of all feasible clusterings can then be described by the set of all integer vectors that satisfy the following constraints

$$\sum_{i=1}^k y_{ij} = 1 \quad \forall j \in [n], \quad (3a)$$

$$\sum_{j=1}^n y_{ij} \geq \kappa_i^- \quad \forall i \in [k], \quad (3b)$$

$$\sum_{j=1}^n y_{ij} \leq \kappa_i^+ \quad \forall i \in [k], \quad (3c)$$

$$y_{ij} \geq 0 \quad \forall i \in [k], j \in [n]. \quad (3d)$$

We refer to the feasible region (3) as a *transportation polytope*. (Note that it shares its constraint matrix, with duplication of some of the rows, with classical transportation problems.) Constraint (3a) ensures that each item is assigned to exactly one cluster. Constraints (3b) and (3c) ensure that the clustering is feasible, i.e., each cluster C_i is assigned between κ_i^- and κ_i^+ items. Note that the constraint matrix on left-hand side of (3) is totally unimodular, and the right-hand side is integer. Thus, the vertices of (3) are integer. Every clustering corresponds to a vertex and vice versa. We will identify the vertices with the encoded clusterings

Let us provide a formal definition, and notation, for these polytopes, as well as for the closely connected class of *partition polytopes*.

Definition 5 (Bounded-Shape Polytopes). *The feasible region of (3) is called the bounded-shape transportation polytope and is denoted by $\mathcal{T}^\pm(X, k, \kappa^-, \kappa^+) = \mathcal{T}^\pm(\kappa^-, \kappa^+)$.*

For a clustering $C = (C_1, \dots, C_k)$, let $w(C) := (\sum_{x \in C_1} x, \dots, \sum_{x \in C_k} x) \in \mathbb{R}^{d \cdot k}$ be the clustering vector of C . We call $\mathcal{P}^\pm(X, k, \kappa^-, \kappa^+) = \mathcal{P}^\pm(\kappa^-, \kappa^+) := \text{conv}(\{w(C) \mid C \text{ is feasible}\})$ the bounded-shape partition polytope.

We will omit κ^- and κ^+ and just write \mathcal{T}^\pm or \mathcal{P}^\pm if the bounds on the cluster sizes are clear from the context.

Informally, clustering vectors $w(C)$ are formed from k vectors, one for each cluster C_i summing up the locations in \mathbb{R}^d of items in the cluster. This allows bounded-shape partition polytopes an encoding of valuable information on the locations of items, in contrast to bounded-shape transportation polytopes which only encode item assignments to the clusters. When we write the data set into the columns of a matrix $M = (x_1, \dots, x_n)$, it is not hard to see that \mathcal{P}^\pm is the image of \mathcal{T}^\pm under the linear map that first transposes the vector $y \in \mathbb{R}^{n \cdot k}$ into an $(n \times k)$ -matrix Y , multiplies

this with M , and rewrites the corresponding matrix $M \cdot Y$ into a column vector. Note that we may assume that the matrix M has full rank equal to d . Otherwise, all items are contained in some affine subspace of \mathbb{R}^d , and we may, w.l.o.g., restrict to this subspace.

Bounded-shape partition polytopes were studied in detail in the literature [3, 8, 9, 15, 14]. There are two choices for κ^\pm that are particularly well-understood, the *single-shape* partition polytopes [5, 8] and the *all-shape* partition polytopes [8, 14]. We define these terms for both partition and transportation polytopes.

Definition 6 (Single-Shape and All-Shape Polytopes). *For $\kappa^- = \kappa^+ = \kappa$, we call $\mathcal{P}^=(\kappa) = \mathcal{P}^\pm(\kappa^-, \kappa^+)$ the single-shape partition polytope and $\mathcal{T}^=$ the corresponding single-shape transportation polytope. For $\kappa^- = (0, \dots, 0)$ and $\kappa^+ = (n, \dots, n)$, we call $\mathcal{P} = \mathcal{P}^\pm(\kappa^-, \kappa^+)$ the all-shape partition polytope and \mathcal{T} the corresponding all-shape transportation polytope.*

There is a close connection between constrained LSAs and the single-shape transportation polytope [5]. Note that computing a constrained LSA to given sites $s_1, \dots, s_k \in \mathbb{R}^d$ is equivalent to minimizing $\sum_{i=1}^k \sum_{j=1}^n \|x_j - s_i\|^2 y_{ij}$ over \mathcal{T}^\pm . If the cluster sizes are fixed, i.e., in the single-shape case, this is equivalent to linear optimization over the single-shape transportation polytope $\mathcal{T}^=$:

$$\sum_{i=1}^k \sum_{j=1}^n \|x_j - s_i\|^2 y_{ij} = \sum_{j=1}^n \|x_j\|^2 \underbrace{\sum_{i=1}^k y_{ij}}_{=1 \text{ (3a)}} - 2 \sum_{i=1}^k \sum_{j=1}^n x_j^T s_i y_{ij} + \sum_{i=1}^k \|s_i\|^2 \underbrace{\sum_{j=1}^n y_{ij}}_{=\kappa_i \text{ (3b), (3c)}}. \quad (4)$$

So minimizing (4) over all $y \in \mathcal{T}^=$ is equivalent to

$$\min_{y \in \mathcal{T}^=} \underbrace{\sum_{j=1}^n \|x_j\|^2 + \sum_{i=1}^k \kappa_i \|s_i\|^2}_{= \text{constant}} - 2 \sum_{i=1}^k \sum_{j=1}^n x_j^T s_i y_{ij} \iff \max_{y \in \mathcal{T}^=} \sum_{i=1}^k \sum_{j=1}^n x_j^T s_i y_{ij}. \quad (5)$$

In the following, we write $c_{ij}(s) = x_j^T s_i$, so it becomes clear that (5) maximizes the linear objective function $c(s) \in \mathbb{R}^{n \cdot k}$ over $\mathcal{T}^=$. (We will continue to use the notation $c(s)$ for such an objective function constructed from a site vector s in the remainder of the paper.) Due to

$$\sum_{i=1}^k \sum_{j=1}^n x_j^T s_i y_{ij} = \sum_{i=1}^k s_i^T \left(\sum_{x_j \in C_i} x_j \right),$$

this is equivalent to a maximization of the linear objective function $s \in \mathbb{R}^{k \cdot d}$, the site vector itself, over $\mathcal{P}^=$. We obtain the following proposition.

Proposition 1 ([5]). *A clustering C is a constrained LSA to the site vector $s \in \mathbb{R}^{d \cdot k}$ if and only if it maximizes $c(s)$ over $\mathcal{T}^=$, respectively if it maximizes s over $\mathcal{P}^=$. Equivalently, there exists a separating power diagram with respect to sites s for C .*

In particular, this means that the vertices of partition polytopes $\mathcal{P}^=$ are in one-to-one correspondence to separable clusterings [3, 15]. In fact, they allow for a separating power diagram where no items are on the boundary of cells [8]. Again, we identify the vertices with their encoded clusterings.

Note that the bounded-shape polytopes are the convex hull of the union over all single-shape polytopes, i.e., $\mathcal{T}^\pm(\kappa^-, \kappa^+) = \text{conv}(\bigcup_{\kappa^- \leq \kappa \leq \kappa^+} \mathcal{T}^=(\kappa))$ and $\mathcal{P}^\pm(\kappa^-, \kappa^+) = \text{conv}(\bigcup_{\kappa^- \leq \kappa \leq \kappa^+} \mathcal{P}^=(\kappa))$,

see [8]. Thus a vertex of the bounded-shape partition polytope is also a vertex of the single-shape partition polytope corresponding to the particular shape of the encoded clustering. This leads to the following proposition.

Proposition 2 ([3, 8]). *Let C be a clustering C and $s \in \mathbb{R}^{d \cdot k}$ be a site vector. If the clustering vector $w(C)$ maximizes s over \mathcal{P}^\pm , then C is a constrained LSA to the site vector s , and there exist a separating power diagram with respect to sites s for C .*

Note that Proposition 2 is not an ‘if and only if’ relationship: a vertex of a single-shape partition polytope $\mathcal{P}^=$ (of a shape allowed by κ^- , κ^+) might not be a vertex of the bounded-shape partition polytope \mathcal{P}^\pm . It may lie on the boundary of \mathcal{P}^\pm or in its strict interior. This distinction will be important throughout this paper.

2.2.2 Adjacency in Bounded-Shape Polytopes

We say that two clusterings are *adjacent* in, e.g., \mathcal{T}^\pm if the corresponding vertices share an edge in the transportation polytope. Borgwardt and Happach [8] gave a necessary condition for two vertices of \mathcal{P}^\pm (i.e., clustering vectors) to be adjacent, and Borgwardt and Viss [9] showed that two clusterings are adjacent in \mathcal{T}^\pm if and only if their CDG contains only a single path or cycle, where the involved clusters are of a certain structure. We say C_i is *free* if $\kappa_i^- < |C_i| < \kappa_i^+$. The following proposition summarizes the results of [8, 9] on the edge structure of the respective polytopes.

Proposition 3 ([8, 9]). *Let $w(C), w(C')$ be two vertices of \mathcal{P}^\pm that share an edge. Then the clustering difference graph $CDG(C, C')$ comprises a single path, a single cycle, or two parallel arcs only.*

Two clusterings C and C' share an edge in \mathcal{T}^\pm if and only if the clustering difference graph $CDG(C, C')$ consists of a single path in which no interior cluster is free or of a single cycle in which at most one cluster is free.

In particular, if two clusterings are adjacent in \mathcal{T}^\pm then their CDG consists of a single path or cycle. (For clusterings adjacent in $\mathcal{T}^=$ or \mathcal{T} , the CDG comprises a single cycle or a single arc, respectively, see [9].) In turn, this means that adjacent clusterings differ by a single cyclical or sequential exchange. This fact will be a valuable tool for our purposes: the bounded-shape transportation polytopes have an explicit algebraic description in the form of the feasible region (3). This will allow us to adapt classical linear programming techniques to design (part of) the desired transition between two separable clusterings.

3 The Overall Transition

Given two separable clusterings, an initial clustering C^s and a target clustering C^t with corresponding sites s and t , our goal is to provide an algorithm that returns a sequence of separable clusterings representing a gradual transition from C^s to C^t . The sequence corresponds to (constrained) LSAs that appear in a linear transition of the sites from s to t . Two consecutive clusterings in this sequence will only differ by a single (cyclical) exchange of items, and cluster sizes will stay between lower and upper bounds given by C^s and C^t throughout. See Section 1.3 for a motivation and justification of these choices for our approach. This section is dedicated to a description how this overarching strategy can be realized through polyhedral theory and methods of linear programming.

In addition to a sequence of constrained LSAs

$$C^1, \dots, C^\eta,$$

our algorithm also returns a sequence of power diagrams

$$P^1, \bar{P}^2, P^2, \bar{P}^3, \dots, P^{\eta-1}, \bar{P}^\eta, P^\eta,$$

where P^ν (uniquely) induces C^ν from the sequence and \bar{P}^ν is a shared power diagram for C^ν and $C^{\nu-1}$, for all $1 \leq \nu \leq \eta$. Throughout the sequence, the site vectors follow a linear transition from sites s to sites t , i.e., $(1-\lambda)s + \lambda t$ for increasing λ . The site vectors of LSAs C^ν and corresponding P^ν will coincide. Consecutive clusterings C^ν and $C^{\nu-1}$ will both be constrained LSAs for the site vector of \bar{P}^ν , i.e., their objective function values with respect to these sites are equally good.

3.1 A Linear Transition between Separable Clusterings

We continue our discussion with a focus on the computation of the sequence of clusterings. We discuss the construction of the associated power diagrams in Section 3.2. First, we describe the main idea of the algorithm.

Let C^s and C^t be the initial and target clustering with site vector s and t , respectively. First, let us assume that C^s and C^t are separable in the sense of [3]. More precisely, we assume they satisfy Proposition 2 with respect to the bounded-shape partition polytope $\mathcal{P}^\pm = \mathcal{P}^\pm(\kappa^-, \kappa^+)$ using cluster size bounds $\kappa_i^- = \min\{|C_i^s|, |C_i^t|\}$ and $\kappa_i^+ = \max\{|C_i^s|, |C_i^t|\}$ for all $i \in [k]$, and we assume the clustering vectors $w(C^s)$ and $w(C^t)$ are on the boundary of \mathcal{P}^\pm in direction of $s \in \mathbb{R}^{d \cdot k}$ and $t \in \mathbb{R}^{d \cdot k}$, respectively. Recall that not all constrained LSAs satisfy this property (even if they were feasible w.r.t. the given κ^\pm).

When moving linearly from the site vector s to t , we obtain a sequence of site vectors of the form $(1-\lambda)s + \lambda t \in \mathbb{R}^{d \cdot k}$ with $\lambda \in [0; 1]$. For every λ , we get a clustering vector $w(C^\lambda)$ that maximizes the objective vector $(1-\lambda)s + \lambda t$ over \mathcal{P}^\pm , where $C^0 = C^s$ and $C^1 = C^t$. That is, the clustering C^λ is separable and is induced by a power diagram with site vector $(1-\lambda)s + \lambda t$.

Recall that an objective vector is maximized at a boundary point x of a d -dimensional polytope P if and only if it is contained in the normal cone $N_P(x) := \{c \in \mathbb{R}^d \mid c^T x \geq c^T x' \ \forall x' \in P\}$. Let C be a clustering that is induced by a power diagram with site vector $\bar{s} \in \mathbb{R}^{d \cdot k}$ and let C' be any other clustering. Let $i(j), i'(j) \in [k]$ be the indices such that $x_j \in C_{i(j)}$ and $x_j \in C'_{i'(j)}$ for all $j \in [n]$. Let $y, y' \in \{0, 1\}^{n \cdot k}$ be the feasible solutions for the bounded-shape transportation polytope \mathcal{T}^\pm that correspond to C and C' , respectively. We have the following equivalence:

$$\begin{aligned} \bar{s} \in N_{\mathcal{P}^\pm}(w(C)) &\iff \bar{s}^T w(C) \geq \bar{s}^T w(C') \iff \sum_{i=1}^k \bar{s}_i^T \left(\sum_{\substack{j \in [n] \\ i=i(j)}} x_j \right) \geq \sum_{i=1}^k \bar{s}_i^T \left(\sum_{\substack{j \in [n] \\ i=i'(j)}} x_j \right) \\ &\iff \sum_{j=1}^n x_j^T \bar{s}_{i(j)} \geq \sum_{j=1}^n x_j^T \bar{s}_{i'(j)} \iff \sum_{i=1}^k \sum_{j=1}^n c(\bar{s})_{ij} y_{ij} \geq \sum_{i=1}^k \sum_{j=1}^n c(\bar{s})_{ij} y'_{ij} \\ &\iff c(\bar{s})^T y \geq c(\bar{s})^T y' \iff c(\bar{s}) \in N_{\mathcal{T}^\pm}(y) \end{aligned}$$

Hence, the clustering vectors $w(C^\lambda)$ are on the boundary of \mathcal{P}^\pm if and only if their 0/1 vectors in \mathcal{T}^\pm are optimal vertices in direction of $c((1-\lambda)s + \lambda t)$. A clustering whose corresponding vertex of \mathcal{T}^\pm is optimal w.r.t. an objective vector $c(\bar{s})$ for some $\bar{s} \in \mathbb{R}^{d \cdot k}$ is called *radial* w.r.t. the site vector \bar{s} . Equivalently, a clustering C is radial w.r.t. \bar{s} if its corresponding clustering vector $w(C)$ contains \bar{s} in its normal cone $N_{\mathcal{P}^\pm}(w(C))$.

Note that $c((1-\lambda)s + \lambda t) = (1-\lambda)c(s) + \lambda c(t)$, so a linear transition from s to t w.r.t. \mathcal{P}^\pm is equivalent to a linear transition from $c(s)$ to $c(t)$ w.r.t. \mathcal{T}^\pm . Thus, instead of moving along

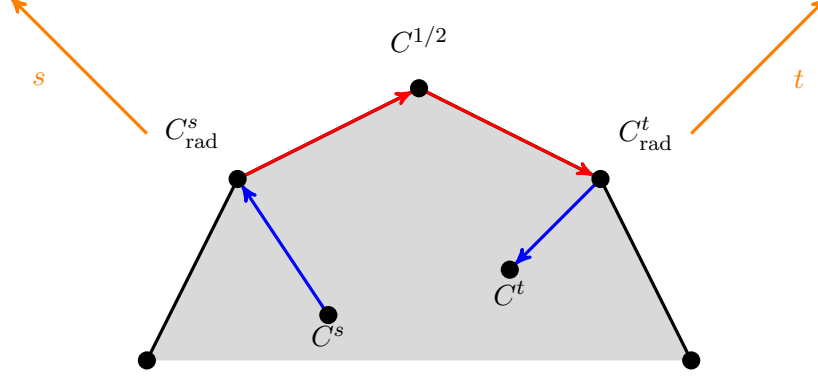
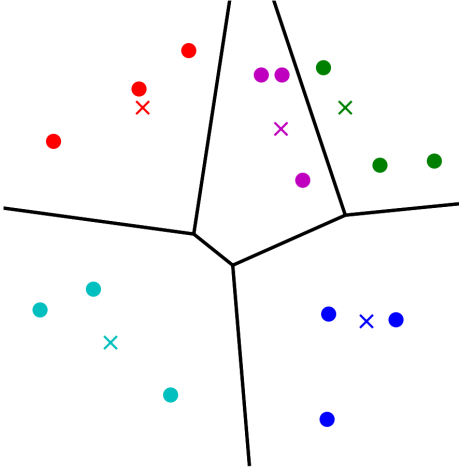


Figure 6: Sketch of a transition from C^s to C^t over \mathcal{P}^\pm . C^s is first transitioned to a radial clustering C^s_{rad} for the same sites; then C^s_{rad} is transitioned into C^t_{rad} , the radial clustering corresponding to C^t , through a walk along the boundary of the polytope; finally C^t_{rad} is transitioned into C^t . The current site vectors stay fixed in the blue part of the transition, and change linearly from s to t in the red part.

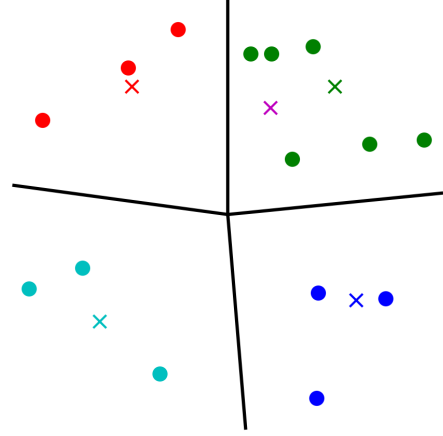
the boundary of the bounded-shape partition polytope, we can move along the boundary of the bounded-shape transportation polytope. Recall that feasible clusterings are in one-to-one correspondence to the vertices of \mathcal{T}^\pm and adjacent vertices differ by a single cyclical or sequential exchange (Proposition 3). This implies that we can perform the walk along the boundary of \mathcal{T}^\pm as an *edge walk*. Further, note we have an explicit, algebraic representation (3) of \mathcal{T}^\pm , so we have all the necessary information for a sensitivity analysis for a current clustering, for example in the form of a simplex tableau for its vertex. This allows us the design of an iterative scheme, much akin to parametric optimization, that finds the values of λ for which the current clustering changes during the transition $(1 - \lambda)s + \lambda t$ (for increasing λ), as well as to identify the exchange of items by which two consecutive clusterings differ. These steps are summarized in `ALGORADTORAD`, see Algorithm 3, which is devised and discussed in Section 5. Geometrically, the algorithm returns a walk along the boundary of \mathcal{P}^\pm , respectively an edge walk in \mathcal{T}^\pm from an initial radial clustering C^s_{rad} to a target radial clustering C^t_{rad} .

Now suppose that the clustering vector of the initial clustering C^s or target clustering C^t is not on the boundary of \mathcal{P}^\pm , i.e., the clustering is not radial. W.l.o.g., we assume that C^s is not radial w.r.t. s . That is, the clustering C^s is a constrained LSA, i.e., a vertex of the corresponding single-shape partition polytope (of all clusterings with the same shape), but the 0/1 vector of C^s is not an optimum vertex of \mathcal{T}^\pm in direction of $c(s)$, and only an optimal vertex of \mathcal{T}^\pm .

In this situation, we first transition C^s into a radial clustering C^s_{rad} w.r.t. s , i.e., a vertex of the bounded-shape transportation polytope in direction of $c(s)$. We do the same for C^t to compute a radial clustering C^t_{rad} . Then we are able to construct a transition from C^s_{rad} to C^t_{rad} in the form of an edge walk in \mathcal{T}^\pm , as before. The computation of a transition from a constrained LSA to a radial clustering is described by `ALGOINITTORAD`, see Algorithm 2, which is devised and discussed in Section 4. In particular, we will show that all intermediate clusterings on the transition from C^s to C^s_{rad} are constrained LSAs w.r.t. the site vector s and can be constructed such that two consecutive clusterings differ by only a single sequential exchange. The same holds for the transition between C^t and C^t_{rad} . Note that the transition from C^t_{rad} to C^t can be computed by applying `ALGOINITTORAD` and reversing the order of the returned sequence of clusterings. We obtain a fixed-site transition for the first and final part of the overall transition.



(a) A radial clustering (single-shape)



(b) A radial clustering (all-shape)

Figure 7: Two radial clusterings. In (a), the computation was done over $\mathcal{T}^=$, i.e., a single-shape transportation polytope. In (b), the computation was done over \mathcal{T} , i.e., the all-shape polytope. Note that (a) is a ‘normal’ constrained LSA, while the clusters in (b) are arranged ‘radially’ around the origin, and there is an empty cluster.

A conceptual sketch of the overall transition from C^s to C^t is shown in Figure 6. The shaded area represents an underlying bounded-shape partition polytope \mathcal{P}^\pm , as well as two site vectors s and t . C^s and C^t are constrained LSAs for these site vectors, but not radial clusterings w.r.t. \mathcal{P}^\pm . The transitions from the initial clustering C^s to its radial clustering C_{rad}^s and from the radial clustering C_{rad}^t to the target clustering C^t are depicted in blue. They begin, respectively stop, at the radial ‘counterparts’ of C^s and C^t . The transition between the two radial clusterings is depicted in red; see above. The intermediate clustering named $C^{1/2}$ is radial w.r.t. \mathcal{P}^\pm to the convex combination $(1 - \lambda)c(s) + \lambda c(t)$ for $\lambda = \frac{1}{2}$.

Let us briefly comment on the role of the radial clusterings as intermediate steps of the transition. Recall that the transition to radial clusterings is necessary such that linear programming methods allow for the computation of a linear transition from initial sites s to target sites t ; see ALGORADTORAD. Radial clusterings, however, are not only LSAs, but optimizers of $c(s)$ over *all* feasible clusterings, i.e., clusterings of all feasible shapes. Some geometric intuition helps understand that having radial clusterings as intermediate steps in our transition is not a significant restriction. Figure 7 shows two examples. In a single-shape setting, *any* LSA is a radial clustering and vice versa, so there is no restriction; see Figure 7(a). In contrast, in the all-shape setting where all clustering shapes are feasible, items x_j are assigned to the sites s_i (and thus cluster C_i) with the largest scalar product $x_j^T s_i$. Thus, the clusters are arranged ‘radially’ around the origin, and it is even possible to get empty clusters; see Figure 7(b). In fact, this geometric observation is the reason for the naming of the term.

Of course, we want to avoid imposing additional structure on the clusterings in our transition. This is achieved directly through the restriction of cluster sizes in our computations: recall that they are performed over $\mathcal{T}^\pm(\kappa^-, \kappa^+)$ with $\kappa_i^- = \min\{|C_i^s|, |C_i^t|\}$ and $\kappa_i^+ = \max\{|C_i^s|, |C_i^t|\}$ for all $i \in [k]$. This means that all intermediate clusterings can only have cluster sizes between the lower and upper bounds induced by C^s and C^t . This is not only a desirable property for the transition itself,

but it also means that all clusterings in the transition – radial or not – are (general) constrained LSAs for prescribed cluster sizes between those of C^s and C^t ; they correspond to optima over some $\mathcal{T}^=$, see Figure 7(a). The only actual restriction happening in view of our transition is that we do not (need to) consider all constrained LSAs (of feasible shapes) to construct it.

Algorithm 1: Linear transition from initial LSA C^s to target LSA C^t .

Input: Initial and target constrained LSAs C^s and C^t w.r.t. site vectors $s \in \mathbb{R}^{d \cdot k}$ and $t \in \mathbb{R}^{d \cdot k}$, respectively.

Output: Sequence of constrained LSAs and sequence of corresponding power diagrams that satisfy the properties of Theorem 1

- 1 Set $\kappa_i^- \leftarrow \min\{|C_i^s|, |C_i^t|\}$ and $\kappa_i^+ \leftarrow \max\{|C_i^s|, |C_i^t|\}$ for all $i \in [k]$;
- 2 Call $\text{ALGOINITTORAD}(C^s, s, \kappa^-, \kappa^+)$ and let $(C^{s,0}, C^{s,1}, \dots, C^{s,p})$ be the returned sequence of clusterings where $C^{s,0} = C^s$ and let $(P^{s,0}, \bar{P}^{s,1}, \dots, \bar{P}^{s,p}, P^{s,p})$ be the returned sequence of power diagrams; set $C_{\text{rad}}^s \leftarrow C^{s,p}$;
- 3 Call $\text{ALGOINITTORAD}(C^t, t, \kappa^-, \kappa^+)$ and let $(C^{t,0}, C^{t,1}, \dots, C^{t,q})$ be the returned sequence of clusterings where $C^{t,0} = C^t$ and let $(P^{t,0}, \bar{P}^{t,1}, \dots, \bar{P}^{t,q}, P^{t,q})$ be the returned sequence of power diagrams; set $C_{\text{rad}}^t \leftarrow C^{t,q}$;
- 4 Call $\text{ALGORADTORAD}(C_{\text{rad}}^s, C_{\text{rad}}^t, s, t, \kappa^-, \kappa^+)$ and let $(C^{\lambda_0}, C^{\lambda_1}, \dots, C^{\lambda_m})$ be the returned sequence of clusterings where $C^{\lambda_0} = C_{\text{rad}}^s$ and $C^{\lambda_m} = C_{\text{rad}}^t$ and let $(\bar{P}^{\lambda_1}, P^{\lambda_1}, \dots, \bar{P}^{\lambda_{m-1}}, P^{\lambda_{m-1}}, \bar{P}^{\lambda_m})$ be the returned sequence of power diagrams;
- 5 **return** sequence of clusterings

$$(C^{s,0}, C^{s,1}, \dots, C^{s,p}, C^{\lambda_1}, \dots, C^{\lambda_m}, C^{t,q-1}, \dots, C^{t,1}, C^{t,0})$$

and sequence of power diagrams

$$(P^{s,0}, \bar{P}^{s,1}, \dots, \bar{P}^{s,p}, P^{s,p}, \bar{P}^{\lambda_1}, \dots, P^{\lambda_{m-1}}, \bar{P}^{\lambda_m}, P^{t,q}, \bar{P}^{t,q}, P^{t,q-1}, \dots, \bar{P}^{t,1}, P^{t,0})$$

Algorithm 1 summarizes our approach for a linear transition from C^s to C^t . We formally state correctness of Algorithm 1, and the many favorable properties of the constructed walk, in the following theorem.

Theorem 1. *Let C^s and C^t be two constrained LSAs with site vectors s and t . Algorithm 1 returns a sequence of clusterings*

$$(C^{s,0}, C^{s,1}, \dots, C^{s,p}, C^{\lambda_1}, \dots, C^{\lambda_m}, C^{t,q-1}, \dots, C^{t,1}, C^{t,0})$$

and a sequence of power diagrams

$$(P^{s,0}, \bar{P}^{s,1}, \dots, \bar{P}^{s,p}, P^{s,p}, \bar{P}^{\lambda_1}, \dots, P^{\lambda_{m-1}}, \bar{P}^{\lambda_m}, P^{t,q}, \bar{P}^{t,q}, P^{t,q-1}, \dots, \bar{P}^{t,1}, P^{t,0})$$

that satisfy the following properties:

1. $C^{s,0} = C^s$, $C^{t,0} = C^t$
2. all clusterings are constrained LSAs (and thus separable)
3. all clusterings have cluster sizes $|C_i|$ satisfying $\kappa_i^- := \min\{|C_i^s|, |C_i^t|\} \leq |C_i| \leq \kappa_i^+ := \max\{|C_i^s|, |C_i^t|\}$ for all $i \leq k$

4. consecutive clusterings in the sequence differ by a single cyclical or sequential exchange of items
5.
 - $P^{s,i}$ is a separating power diagram for sites s for $C^{s,i}$
 - P^{λ_i} is a separating power diagram for C^{λ_i}
 - $P^{t,i}$ is a separating power diagram for sites t for $C^{t,i}$
6.
 - for each pair of consecutive clusterings $C^{s,i-1}, C^{s,i}$, \bar{P}^i is a shared power diagram for sites s
 - for each pair of consecutive clusterings $C^{\lambda_i}, C^{\lambda_{i+1}}$, \bar{P}^{λ_i} is a shared power diagram for sites $(1 - \lambda_i)s + \lambda_i t$
 - for each pair of consecutive clusterings $C^{t,i}, C^{t,i-1}$, \bar{P}^i is a shared power diagram for sites s
7. $C_{\text{rad}}^s = C^{s,p} = C^{\lambda_0}, C^{\lambda_1}, \dots, C^{\lambda_m} = C^{t,q} = C_{\text{rad}}^t$ are radial clusterings for sites $(1 - \lambda_i)s + \lambda_i t$ for all $i \geq 0$ w.r.t. $\mathcal{P}^\pm(\kappa^-, \kappa^+)$ and $\mathcal{T}^\pm(\kappa^-, \kappa^+)$ (with κ^\pm as defined in 3.)
8. $C^{s,0}, C^{s,1}, \dots, C^{s,p}$ are constrained LSAs for sites s
9. $C^{t,q-1}, \dots, C^{t,1}, C^{t,0}$ are constrained LSAs for sites t
10. the shapes $|C^{s,i}|$ of $C^{s,0}, C^{s,1}, \dots, C^{s,p}$ are all distinct; the number of clusterings in this part of the sequence is bounded by the number of shapes
11. the shapes $|C^{t,q}|$ of $C^{t,q}, C^{t,q-1}, \dots, C^{t,0}$ are all distinct; the number of clusterings in this part of the sequence is bounded by the number of shapes

Proof. Recall the informal description of the algorithm above. Note that Algorithm 1 essentially consists of two calls to `ALGOINITTORAD` (lines 2 and 3) and a call to `ALGORADTORAD` (line 4). The two calls to `ALGOINITTORAD` provide a transition of C^s into radial C_{rad}^s and C^t into radial C_{rad}^t . The call to `ALGORADTORAD` provides a transition of C_{rad}^s to C_{rad}^t . Along with these sequences of clusterings, a corresponding sequence of power diagrams is computed. The returned walk is a concatenation of the sequence of clusterings from C^s to C_{rad}^s (line 2), from C_{rad}^s to C_{rad}^t (line 4), and from C_{rad}^t to C^t (line 3). The latter is a simple reversal of the transition from C^t into radial C_{rad}^t computed in line 3. The order for the calls to the algorithms, in particular the call to `ALGOINITTORAD` in line 3 before the call to `ALGORADTORAD` in line 4, is based on the fact that `ALGORADTORAD` requires C_{rad}^t as input, and C_{rad}^t is found as a part of the earlier run of `ALGOINITTORAD`.

The claimed properties of the constructed sequence of clusterings are now a direct consequence of correctness, and precisely these properties, of the three parts of the walk. We prove correctness of `ALGOINITTORAD` in Theorem 2 and correctness of `ALGORADTORAD` in Theorem 3.

Claim 1 (in this theorem) corresponds to Property 1 in Theorem 2. Claims 2 to 6 follow from Properties 2 to 6, respectively, in Theorems 2 and 3. Claim 7 follows from Property 1 in Theorem 2 and Property 2 in Theorem 2. Claims 8 and 9 correspond to Property 2 in Theorem 2, and Claims 10 and 11 correspond to Property 7 in Theorem 2. \square

Note that some of the steps in Algorithm 1 can be simplified if the bounds on the cluster sizes κ^- and κ^+ are not arbitrary. If $\kappa^- = \kappa^+$, then Proposition 1 yields that a clustering is an LSA

w.r.t. a site vector $a \in \mathbb{R}^{d \cdot k}$ if and only if it is radial w.r.t. a . Hence, if the cluster sizes of the initial and target clustering coincide, we get $C^s = C_{\text{rad}}^s$ and $C^t = C_{\text{rad}}^t$, so we can omit `ALGOINITTORAD`. In the all-shape case, i.e., when $\kappa^- = (0, \dots, 0)$ and $\kappa^+ = (n, \dots, n)$, radial clusterings have a special, simple form (see Figure 7(b)), and the algebra for the transition between radial clusterings becomes especially simple.

3.2 Computation of Separating Power Diagrams

In addition to the construction of a sequence of clusterings, we construct a sequence of corresponding separating power diagrams. Let ν be an iterator for the sequence of clusterings. The power diagrams are of two types: power diagrams $P^\nu = P^{s,i}, P^{\lambda_i}, P^{t,i}$ are supposed to be ‘good’ power diagrams inducing clustering $C^\nu = C^{s,i}, C^{\lambda_i}, C^{t,i}$ in the sequence (and no other clusterings from the sequence); power diagrams $\bar{P}^\nu = \bar{P}^i, \bar{P}^{\lambda_i}$ are shared for two consecutive clusterings $C^{\nu-1}$ and C^ν , inducing both $C^{s,i-1}, C^{s,i}$ or $C^{t,i}, C^{t,i-1}$, respectively $C^{\lambda_i}, C^{\lambda_{i+1}}$, depending on the part of the sequence. In this section, we discuss the computation of these power diagrams.

To this end, recall from Proposition 2 that for every clustering C with clustering vector $w(C)$ on the boundary of \mathcal{P}^\pm or $\mathcal{P}^=$, and every vector $\bar{s} \in \mathbb{R}^{d \cdot k}$ that is contained in the normal cone at $w(C)$, there exists a power diagram for site vector \bar{s} that induces the clustering C . The scalars $\gamma_1, \dots, \gamma_k$ in our first definition of a power diagram, see Equation (1), and hence also the weights in the equivalent Definition 3, only depend on X and \bar{s} and can be constructed for any \bar{s} in the normal cone [3, 5, 12].

Let us first discuss the construction of a ‘good’ power diagram P^ν that induces clustering C^ν in the sequence: we want a good site vector, and good positions of the separating hyperplanes. First, note that we are given a site vector in the normal cone for every clustering C^ν . For the clusterings $C^{s,0}, \dots, C^{s,p}$ and $C^{t,q}, \dots, C^{t,0}$ (blue arcs in Figure 6) that are returned by `ALGOINITTORAD`, we know that s and t are contained in the normal cone of the clustering vector in the respective single-shape partition polytopes. For the clusterings C^{λ_r} ($1 \leq r \leq m$) along the linear transition $(1 - \lambda)s + \lambda t$ (red arcs in Figure 6), the value $\lambda_r \in [0; 1]$ is chosen such that $s^{\lambda_r} = (1 - \lambda_r)s + \lambda_r t$ is contained in the intersection of the normal cones of $w(C^{\lambda_{r-1}})$ and $w(C^{\lambda_r})$, as we will see in `ALGORADTORAD` and Section 5. Hence, a natural choice of a site vector that is in the normal cone at $w(C^{\lambda_r})$, but not in the normal cone of the previous or next clustering vector, is a convex combination of s and t in the form $\frac{1}{2}(s^{\lambda_r} + s^{\lambda_{r+1}})$ for $1 \leq r < m$. Note that this choice of site vector for C^{λ_r} implies that the constructed power diagram uniquely induces C^{λ_r} from the sequence. (Recall that the clustering vectors of the first and last clustering of this sequence $C^{\lambda_0} = C_{\text{rad}}^s$ and $C^{\lambda_m} = C_{\text{rad}}^t$ contain s and t in their normal cone by construction, respectively.) Summing up, there is a natural choice for the site vector for each power diagram P^ν . These follow a linear transition from s to t .

Second, we also want good positions of the separating hyperplanes in the underlying space. A common approach in the construction of a separating power diagram is to maximize the so-called *margin*, i.e., maximize the minimum Euclidean distance of any item to the boundary of its cell; see, e.g., [4, 7]. In this paper, we are going to use the given site vectors in the linear transition from s to t ; see above. However, we would like to note that a more general choice would be possible: *any* site vector from the normal cone of clustering vector $w(C)$ with respect to an underlying single-shape partition polytope $\mathcal{P}^=$ would be possible. A central site vector in this normal cone, i.e., one with a maximal distance to the boundary of the normal cone is a best choice in view of the margin (under some mild assumptions) [8]; however, the computation of such a site vector is computationally expensive.

It remains to address the actual computation of a (maximum-margin) power diagram for a given site vector. Given a clustering C and a site vector $\bar{s} = (\bar{s}_1, \dots, \bar{s}_k) \in N_{\mathcal{P}=\{|C| \}}(w(C))$, we can maximize the margin of a power diagram with site vector \bar{s} by solving the following linear program [4, 7]:

$$\max \quad \varepsilon \quad (6a)$$

$$\text{s.t.} \quad \frac{\bar{s}_\ell - \bar{s}_i}{\|\bar{s}_\ell - \bar{s}_i\|}^T x_j + \varepsilon \leq \frac{\gamma_\ell - \gamma_i}{\|\bar{s}_\ell - \bar{s}_i\|} \quad \forall i \in [k], \forall \ell \in [k] \setminus \{i\}, \forall x_j \in C_i, \quad (6b)$$

$$\gamma_1 = 0, \quad (6c)$$

$$\gamma_i \in \mathbb{R} \quad \forall i \in [k], \quad (6d)$$

$$\varepsilon \geq 0. \quad (6e)$$

Note that LP (6) has a feasible solution if and only if there exists a power diagram that induces C . By previous observations, LP (6) has a feasible solution, and for $\varepsilon > 0$ no item is on the boundary of the cell of the resulting power diagram. In fact, because of the scaling by $\|\bar{s}_\ell - \bar{s}_i\|^{-1}$ in (6b), ε corresponds to the minimal *Euclidean* distance of an item to the boundary of its cell. We can simplify the LP if we first compute $\max_{x_j \in C_i} (\bar{s}_\ell - \bar{s}_i)^T x_j$ for all $i \in [k]$ and $\ell \in [k] \setminus \{i\}$, and use this term in the constraints (6b). The resulting LP takes the smaller and simpler form

$$\max \quad \varepsilon \quad (7a)$$

$$\text{s.t.} \quad \frac{\max_{x_j \in C_i} (\bar{s}_\ell - \bar{s}_i)^T x_j}{\|\bar{s}_\ell - \bar{s}_i\|} + \varepsilon \leq \frac{\gamma_\ell - \gamma_i}{\|\bar{s}_\ell - \bar{s}_i\|} \quad \forall i \in [k], \forall \ell \in [k] \setminus \{i\}, \quad (7b)$$

$$\gamma_1 = 0, \quad (7c)$$

$$\gamma_i \in \mathbb{R} \quad \forall i \in [k], \quad (7d)$$

$$\varepsilon \geq 0. \quad (7e)$$

Further, recall that $\gamma_i = \frac{1}{2}(\|\bar{s}_i\|^2 - w_i)$ for some weight vector $w = (0, w_2, \dots, w_k)$, so that a representation of the power diagram following Definition 3 is a simple byproduct.

Finally, for the construction of the shared power diagram \bar{P}^ν that induces both $C^{\nu-1}$ and C^ν , suppose we are given a site vector $\bar{s} \in \mathbb{R}^{d \cdot k}$ that is contained in the intersection of the normal cones of $w(C^{\nu-1})$ and $w(C^\nu)$. For the clusterings $C^{\lambda_r}, C^{\lambda_{r-1}}$ ($1 \leq r \leq m$) along the linear transition $(1 - \lambda)s + \lambda t$ (red arcs in Figure 6), we can choose the site vector $\bar{s} = s^{\lambda_r} = (1 - \lambda_r)s + \lambda_r t$ for P^{λ_r} , see ALGORADTORAD. For two consecutive clusterings in $\{C^{s,0}, \dots, C^{s,p}\}$ and $\{C^{t,q}, \dots, C^{t,0}\}$ (blue arcs in Figure 6), $\bar{s} \in \{s, t\}$ allows the computation of a shared power diagram, too. The somewhat technical proof of this claim is part of the proof of Theorem 2 in Section 4.

In both situations, we obtain a shared power diagram that induces $C^{\nu-1}$ and C^ν by adding the constraints (7b) for $C^{\nu-1}$ to LP (7) for C^ν . Recall that two consecutive clusterings differ by a single cyclical or sequential exchange of items. The items that move from one cluster to another are on the boundary of the respective cells, see [5, 8]. Thus, the optimal objective value of LP (7) is equal to zero and computing a power diagram that induces both clusterings simultaneously can be done by finding a feasible solution $\gamma = (\gamma_1, \dots, \gamma_k)$ to the following set of linear constraints that

do *not* contain a scaling by $\|\bar{s}_\ell - \bar{s}_i\|^{-1}$:

$$\max_{x_j \in C_i^\nu} (\bar{s}_\ell - \bar{s}_i)^T x_j \leq \gamma_\ell - \gamma_i \quad \forall i \in [k], \forall \ell \in [k] \setminus \{i\}, \quad (8a)$$

$$\max_{x_j \in C_i^{\nu-1}} (\bar{s}_\ell - \bar{s}_i)^T x_j \leq \gamma_\ell - \gamma_i \quad \forall i \in [k], \forall \ell \in [k] \setminus \{i\}, \quad (8b)$$

$$\gamma_1 = 0, \quad (8c)$$

$$\gamma_i \in \mathbb{R} \quad \forall i \in [k], \quad (8d)$$

This system can be considered an LP with trivial objective function $\max 0^T \gamma$. Note that, for fixed $i \in [k]$ and $\ell \in [k] \setminus \{i\}$, only the right-hand sides of constraints (8a) and (8b) differ, namely in the maximum of $(\bar{s}_\ell - \bar{s}_i)^T x_j$ over all x_j contained in that respective cluster. The same holds for LP (7) if we drop the scaling by $\|\bar{s}_\ell - \bar{s}_i\|^{-1}$ (and scale ϵ appropriately, too). Thus, the duals of the respective LPs only differ in their objective function. Hence, we do not have to solve all the LPs from scratch in our algorithms, but we can use the previous feasible solution (of the dual) as a warm start.

4 A Fixed-Site Transition between LSAs and Radial Clusterings

In this section, we provide an algorithm called `ALGOINITTORAD` to transition from a constrained LSA w.r.t. some site vector $\bar{s} \in \mathbb{R}^{d \cdot k}$ to a radial clustering w.r.t. \bar{s} . This algorithm can be seen as a pre-processing step for the linear transition along radial clusterings from an initial site vector s to a target site vector t , which is discussed in Section 5. Recall from Section 2 that we do not have an explicit algebraic representation of the bounded-shape partition polytope \mathcal{P}^\pm , which is why we perform the computations over the corresponding bounded-shape transportation polytope \mathcal{T}^\pm . We enter the algorithm with cluster size bounds as part of the input; see lines 2 and 3 of Algorithm 1. If the lower and upper bounds of the cluster sizes coincide, i.e., $\kappa^- = \kappa^+$, the constrained LSA is already radial (Proposition 1), and the pre-processing described in this section is not necessary.

To ensure separability of all intermediate clusterings in the transition, we repeat the following steps: The initial clustering C is a vertex of the bounded-shape transportation polytope \mathcal{T}^\pm . First, we walk along an improving edge in \mathcal{T}^\pm to an adjacent vertex. This vertex corresponds to a better (w.r.t. the objective vector $c(\bar{s})$) clustering C' of different shape. (Note C already was a constrained LSA, i.e., optimal over all clusterings of the same shape.) Then, we fix the lower and upper bounds of the cluster sizes to $|C'|$ and transition in the corresponding single-shape transportation polytope $\mathcal{T}^=(|C'|)$ until we reach an optimal clustering with shape $|C'|$ in direction of $c(\bar{s})$, i.e., a constrained LSA w.r.t. s for shape $|C'|$. As we will show in Lemma 1 and explain in the paragraph following it, there exists such an optimal clustering that differs from the initial clustering C by a single sequential exchange, and it is easy to devise it from C' . Not only does this mean we take a step of the desired form, but it also makes it possible to compute a shared separating power diagram for two consecutive clusterings; we prove this as part of Theorem 2. This concludes the first iteration.

We update the initial clustering from C to C' and repeat this scheme, until we reach a clustering that maximizes $c(s)$ over \mathcal{T}^\pm , i.e., the desired radial clustering. See `ALGOINITTORAD`, Algorithm 2, for a description of this scheme in pseudocode. For a simple wording in the pseudocode, we equate vertices of a bounded-shape transportation polytope and clusterings; recall that they are in one-to-one correspondence. Figure 8 depicts an initial and target clustering, as well as an intermediate clustering in the transition. Note that each clustering C^r ($r \geq 1$) is a constrained LSA w.r.t. \bar{s} for its own shape $|C^r|$, as we optimize over the single-shape transportation polytope in line 4 in

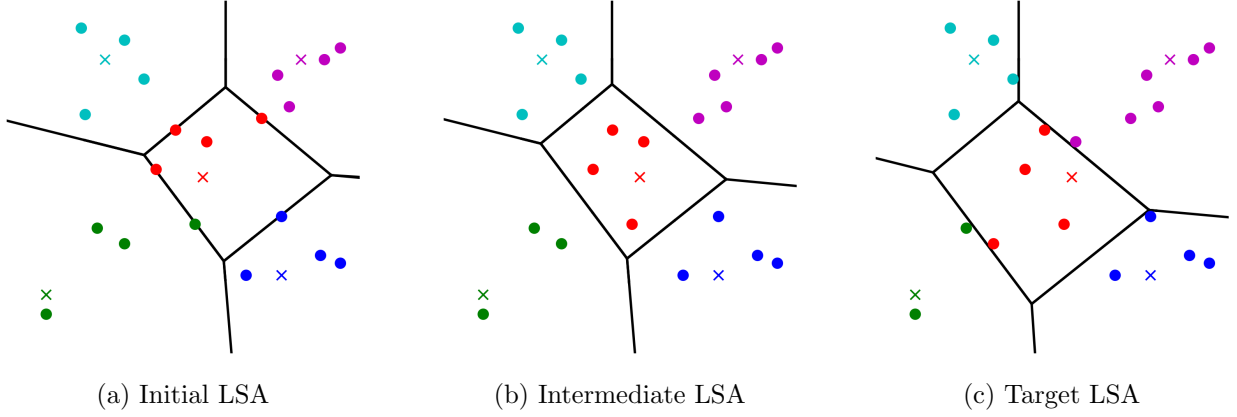


Figure 8: Initial, target, and one intermediate LSA in a fixed-site transition as in `ALGOINITTORAD`. The target LSA is a radial clustering for the (implicit) cluster size bounds. The three clusterings are constrained LSAs for the same sites, but different shapes.

direction of $c(\bar{s})$ in each iteration. Because of this, we call the constructed sequence a *fixed-site transition*. Further, note that the shape of the current clustering changes in each iteration of the while-loop due to the simplex step in line 3. This implies that no two clusterings in the sequence returned by `ALGOINITTORAD` have the same shape.

We sum up the favorable properties of the algorithm, and its output, in the following theorem.

Theorem 2. *Let $C^{\bar{s}}$ be a constrained LSA with site vector \bar{s} , and let κ^-, κ^+ be cluster size bounds such that $\kappa^- \leq |C| \leq \kappa^+$. `ALGOINITTORAD` returns a sequence of clusterings*

$$(C^0, C^1, \dots, C^r)$$

and a sequence of power diagrams

$$(P^0, \bar{P}^1, P^1, \dots, \bar{P}^r, P^r)$$

that satisfy the following properties:

1. $C^0 = C^{\bar{s}}$; C^r is a radial clustering for sites \bar{s}
2. all clusterings are constrained LSAs for sites \bar{s}
3. all clusterings have cluster sizes $|C_i|$ satisfying $\kappa_i^- \leq |C_i| \leq \kappa_i^+$ for all $i \leq k$
4. consecutive clusterings in the sequence differ by a single sequential exchange of items
5. P^i is a separating power diagram for sites \bar{s} for C^i
6. for each pair C^{i-1}, C^i of consecutive clusterings, \bar{P}^i is a shared power diagram for sites \bar{s}
7. the shapes $|C^i|$ are all distinct; the number of clusterings in the sequence is bounded by the number of shapes

Algorithm 2: ALGOINITTORAD($C, \bar{s}, \kappa^-, \kappa^+$). Fixed-site transition from initial LSA w.r.t. site vector \bar{s} to corresponding radial clustering.

Input: Constrained LSA C w.r.t. a site vector $\bar{s} \in \mathbb{R}^{d \cdot k}$; cluster size bounds κ^\pm

Output: Sequence of constrained LSAs and sequence of corresponding power diagrams that satisfy the properties of Theorem 2

```

1  $r \leftarrow 0$  and  $C^0 \leftarrow C$ ;
2 while  $C^r$  is not optimal in  $\mathcal{T}^\pm(\kappa^-, \kappa^+)$  in direction of  $c(\bar{s})$  do
3   Perform a simplex step from  $C^r$  w.r.t. objective  $\max c(\bar{s})^T y$  in  $\mathcal{T}^\pm(\kappa^-, \kappa^+)$  to an
   adjacent vertex/clustering; update  $C$  to the new clustering;
4   Find an optimal clustering in  $\mathcal{T}^-(|C|)$  that differs from  $C^r$  by a single sequential
   exchange; update  $C$  to the new clustering;
5   Solve LP (7) with  $\bar{s}$  and let  $P^r$  be the corresponding power diagram;
6   if  $r \geq 1$  then
7     Compute a feasible solution for (8) with  $\bar{s}$  and  $C^\nu = C$ ,  $C^{\nu-1} = C^{r-1}$ , and let  $\bar{P}^r$ 
     be the corresponding power diagram;
8   end
9    $r \leftarrow r + 1$  and  $C^r \leftarrow C$ ;
10 end
11 return sequence of clusterings  $(C^0, C^1, \dots, C^r)$ 
    and sequence of power diagrams  $(P^0, \bar{P}^1, P^1, \dots, \bar{P}^r, P^r)$ 

```

Proof. Recall the informal description of ALGOINITTORAD above. Most of the claimed properties are direct consequences of the design of the algorithm:

The initial clustering $C^0 = C$ is a constrained LSA w.r.t. \bar{s} . This is equivalent to C^0 being optimal over $\mathcal{T}^-(|C^0|)$, the single-shape transportation polytope of all clusterings of the same shape. Each other clustering C in the produced sequence is computed as an optimum w.r.t. $c(\bar{s})$ over $\mathcal{T}^-(|C|)$ (line 4), and thus also is a constrained LSA w.r.t. s .

The improving Simplex step in line 3 guarantees that each consecutive clustering C is strictly better w.r.t. $c(\bar{s})$. Each clustering is an optimum w.r.t. $c(s)$ over $\mathcal{T}^-(|C|)$, so this strict improvement can only come from finding a clustering of a new shape that is distinct from the shapes of all previous clusterings in the sequence. Thus the sequence of clusterings is finite; in fact, it is bounded by the number of possible shapes. The algorithm terminates with a radial clustering C^r after r runs of the while-loop. This proves properties 1, 2, and 7.

Further, line 3 is the only step that can change the clustering shape. As the simplex step is taken over $\mathcal{T}^\pm(\kappa^-, \kappa^+)$, cluster sizes $|C_i|$ are bounded throughout by $\kappa_i^- \leq |C_i| \leq \kappa_i^+$ for all $i \leq k$. This gives property 3.

We will show property 4, i.e., the fact that two consecutive clusterings only differ by a single sequential exchange of items, in Lemma 1 below.

Property 5 follows immediately from each clustering C^i in the sequence being optimal for sites \bar{s} over $\mathcal{T}^-(|C^i|)$. LP (7) has a feasible solution and returns the desired P^i .

It remains to prove property 6. Let C^{i-1} and C^i denote two consecutive clusterings. Recall

that a clustering C allows a separating power diagram for sites \bar{s} if the vector \bar{s} lies in the normal cone of the clustering vector $w(C)$ in any partition polytope [5]. In fact, this property also holds for *fractional* clusterings, where items can be assigned partially to multiple clusters (adding up to 1) and the corresponding partition polytopes [12].

We have to show that there exists a *shared* power diagram that induces both C^{i-1} and C^i for sites \bar{s} . Let y^{i-1} and y^i be the 0/1-vectors corresponding to C^{i-1} and C^i . Recall that C^{i-1} and C^i only differ by a single sequential exchange of items (property 4). Consider the fractional clustering C^{frac} corresponding to $y^{\text{frac}} = \frac{1}{2}(y^{i-1} + y^i)$. The vector y^{frac} has components 0, 0.5, or 1, and is informally obtained from applying ‘half’ of the sequential exchange applied to C^{i-1} : each item moved now belongs 50% to its original cluster in C^{i-1} and 50% to its new cluster in C^i – the corresponding variables in y^{frac} are 0.5.

Let θ^\pm and η^\pm be cluster size bounds derived as $\theta_i^- = \min\{|C_i^{i-1}|, |C_i^i|\}$, $\theta_i^+ = \max\{|C_i^{i-1}|, |C_i^i|\}$, and $\eta_i^\pm = \max\{|C_i^{i-1}|, |C_i^i|\}$ for all $i \in [k]$. Recall C^{i-1} is optimal w.r.t \bar{s} over $\mathcal{P}(|C^{i-1}|)$, As C^i is optimal w.r.t. \bar{s} over $\mathcal{P}^\pm(\theta^-, \theta^+)$, C^{frac} is optimal w.r.t \bar{s} over $\mathcal{P}^\pm(\theta^-, \eta^+)$. In fact, the same sequential exchange used to obtain C^i from C^{i-1} (recall property 4) leads to the new optimal fractional clustering C^{frac} when moving only 50% of each item involved. This implies the existence of a separating power diagram \bar{P}^i for sites \bar{s} for the fractional clustering C^{frac} . This power diagram \bar{P}^i induces both C^{i-1} and C^i , so it is the desired shared power diagram. For consecutive clusterings C^{i-1} and C^i , such a power diagram \bar{P}^i is found through a solution of LP (8) with sites \bar{s} and $\nu = i$, and denoted in lines 6 to 8 of ALGOINITTORAD. This proves the claim. \square

To complete the proof of Theorem 2, it remains to prove correctness of property 4. We do so in the following lemma. In particular, it shows that the choice of C in line 4 is well-defined: there always exists an optimal constrained LSA for the new clustering shapes identified in line 3 such that the difference to the previous clustering is only a single sequential exchange.

Lemma 1. *Let $\bar{s} \in \mathbb{R}^{d \cdot k}$ be a site vector and consider the i -th iteration of ALGOINITTORAD. Let C^{i-1} refer to the constrained LSA from the previous iteration, and let C correspond to the clustering of updated shape (line 3 of ALGOINITTORAD). There exists a constrained LSA C^i w.r.t. \bar{s} in $\mathcal{T}^\pm(|C|)$ such that $CDG(C^{i-1}, C^i)$ consists of a single path, i.e., such that C^{i-1} and C^i differ by a single sequential exchange of items.*

Proof. For a simple wording, we will indicate that a clustering is optimal over some transportation polytope w.r.t $c(\bar{s})$ by saying it is optimal over the polytope.

We begin the i -th iteration of ALGOINITTORAD with C^{i-1} , which is optimal over $\mathcal{T}^\pm(|C^{i-1}|)$. Clustering C , as devised in line 3 of the algorithm, is of different shape and of strictly better objective function value than C^{i-1} . Let y^{i-1} and y be the 0/1 vectors in \mathcal{T}^\pm corresponding to C^{i-1} and C , respectively. By Proposition 3, we get that $CDG(C^{i-1}, C)$ contains a single path P , which, w.l.o.g., starts at cluster 1 and ends at cluster k . If C is optimal over $\mathcal{T}^\pm(|C|)$, we set $C^i = C$ and are done.

So suppose C is not optimal over $\mathcal{T}^\pm(|C|)$. This means there exists a different optimal clustering C^{opt} over $\mathcal{T}^\pm(|C|)$ with $|C^{\text{opt}}| = |C|$ and corresponding y^{opt} satisfying $c(\bar{s})^T(y^{\text{opt}} - y) > 0$. Consider $CDG(C^{i-1}, C^{\text{opt}})$. Note all nodes in $\{2, \dots, k-1\}$ have even degree and the nodes 1 and k have odd degree. Hence, $CDG(C^{i-1}, C^{\text{opt}})$ greedily decomposes into a path \bar{P} from node 1 to k and a set of arc-disjoint cycles \mathcal{CY} (that also are arc-disjoint from \bar{P}) [6, 9].

Let $y(\mathcal{CY}) := y^{\text{opt}} - y^i \in \{-1, 0, 1\}^{n \cdot k}$; it has components $y_{lj} = -1$ and $y_{lj} = 1$ if and only if there is a cycle in the set \mathcal{CY} that contains an arc (l, ℓ) with label x_j . We use the same notation $y(\mathcal{CY}_v)$ for single cycles \mathcal{CY}_v from \mathcal{CY} and the path \bar{P} , too. The entries of $y(\mathcal{CY})$, respectively

$y(\mathcal{CY}_v)$ or $y(\bar{P})$, represent the removal of item x_j from cluster C_l^{i-1} and addition of it to cluster C_ℓ^{opt} .

Note that $c(\bar{s})^T y(\mathcal{CY}_t) \leq 0$ for any cycle \mathcal{CY}_t from \mathcal{CY} ; otherwise C^{i-1} would not have been optimal over $\mathcal{T}^=(|C^{i-1}|)$. Thus in particular $c(\bar{s})^T y(\mathcal{CY}) \leq 0$. By applying the sequential exchange corresponding to \bar{P} to C^{i-1} , we obtain a clustering C^i with $|C^i| = |C^{\text{opt}}|$ and corresponding y^i satisfying

$$c(\bar{s})^T (y^{\text{opt}} - y^{i-1}) = c(\bar{s})^T (y(\bar{P}) + y(\mathcal{CY})) \leq c(\bar{s})^T y(\bar{P}) = c(\bar{s})^T (y^i - y^{i-1})$$

and thus

$$c(\bar{s})^T (y^i - y^{\text{opt}}) \geq 0$$

As C^{opt} was optimal over $\mathcal{T}^=(|C|)$, C^i is optimal, too. In fact, the inequality is satisfied with equality. C^i differs from C^{i-1} by a single sequential exchange. This proves the claim. \square

The proof shows that finding the next clustering C^i in the sequence (i.e., line 4 of ALGOINITTORAD) can be done by computing an optimal clustering C^{opt} using the simplex method over $\mathcal{T}^=(|C|)$ (starting from C from line 3), then setting up $CDG(C^{i-1}, C^{\text{opt}})$ and greedily deleting all cycles from it, and finally applying the single sequential exchange corresponding to the only remaining path \bar{P} in the CDG to clustering C^{i-1} .

By Proposition 1, each clustering C^i is a constrained LSA w.r.t. the site vector \bar{s} for all $1 \leq i \leq r$. That is, each of the clusterings in (C^0, C^1, \dots, C^r) in ALGOINITTORAD, and hence each of the clusterings in the subsequences $(C^{s,0}, C^{s,1}, \dots, C^{s,p})$ and $(C^{t,q}, C^{t,q-1}, \dots, C^{t,0})$ returned by Algorithm 1, is separable, and in particular a constrained LSA (recall that $C^{s,0} = C^s$ and $C^{t,0} = C^t$) for sites s , respectively t . Further, for all $p, q \geq 1$, the clustering $C^{s,p}$ and $C^{t,q}$ differs from $C^{s,p-1}$ and $C^{t,q-1}$ by a single sequential exchange, respectively.

Summing up, ALGOINITTORAD finds the desired fixed-site transition from a general constrained LSA to a radial clustering, which is used as the first and final part of the overall transition in Theorem 1 and Algorithm 1.

5 A Linear Transition between Radial Clusterings

In this section, we devise an algorithm called ALGORADTORAD to compute a transition between two radial clusterings C_{rad}^s and C_{rad}^t . Each step of the transition corresponds to a single exchange of items, and each intermediate clustering is a radial clustering itself.

Geometrically, both C_{rad}^s and C_{rad}^t lie on the boundary of \mathcal{P}^\pm (for cluster size bounds κ^\pm induced by C_{rad}^s and C_{rad}^t) and the transition forms a walk along the boundary of this polytope. The sequence of clusterings follows the linear transition $(1 - \lambda)s + \lambda t$ of site vectors for increasing λ . In the corresponding \mathcal{T}^\pm , C_{rad}^s and C_{rad}^t are vertices and the transition takes the form an edge walk, following a linear transition of objective functions $(1 - \lambda)c(s) + \lambda c(t)$ for increasing λ . For this transition, we need to identify when and how clusterings change. By performing our computations over \mathcal{T}^\pm (for which there exists an explicit representation), this can be done by adapting classical tools of sensitivity analysis (and parametric programming).

A brief review of ranging. As a service to the reader, let us recall some necessary basics of sensitivity analysis, following notation in [17]. Consider a linear program in standard form given as

$$\begin{aligned} \min \quad & c^T x \\ \text{subject to} \quad & Ax = b \\ & x \geq 0. \end{aligned}$$

Let x^* be an optimal vertex with objective function value $c^T x^* = \zeta^*$, and let a corresponding optimal split of the matrix A into basis- and nonbasis- parts be denoted as (B, N) . We call B the optimal basis.

Informally, sensitivity analysis involves studies of a simplex dictionary (or simplex tableau) for x^* to gain an understanding of how changes to constraints or objective function interact with the optimal basis. For our purposes, we require a particularly simple variation in the form of *ranging*: given a change to the objective function c in the form of $c + \lambda \Delta c$ for some $\lambda \in \mathbb{R}$, we have to devise upper (and lower) bounds on λ at which the current optimal basis is left.

Recall that LP optimality requires primal and dual feasibility. We use x_B to denote the primal basic variables and z_N to denote the dual nonbasic variables (and again use stars to indicate values for the optimum). With this notation, the information in an optimal dictionary is

$$\begin{aligned}\zeta &= \zeta^* - z_N^{*T} x_N \\ x_B &= x_B^* - B^{-1} N x_N.\end{aligned}$$

with

$$\begin{aligned}x_B^* &= B^{-1} b \\ z_N^* &= (B^{-1} N)^T c_B - c_N \\ \zeta^* &= c_B^T B^{-1} b.\end{aligned}$$

A change in the objective function c implies a change of z_N^* and ζ^* , but does not affect x_B^* . By changing c to $c + \lambda \Delta c$, z_N^* increases by $\lambda \Delta z_N$, with

$$\Delta z_N = (B^{-1} N)^T \Delta c_B - \Delta c_N.$$

The current basis remains dual feasible (and thus optimal) as long as $z_N^* + \lambda \Delta z_N \geq 0$. With a case distinction on the sign of λ , one obtains an explicit range of objective functions $c + \lambda \Delta c$ that retain the current optimal basis in the form

$$\left(\min_{j \in N} -\frac{\Delta z_j}{z_j^*} \right)^{-1} \leq \lambda \leq \left(\max_{j \in N} -\frac{\Delta z_j}{z_j^*} \right)^{-1}.$$

This general ranging formula transfers to our setting.

Adaptation to an iterative scheme over \mathcal{T}^\pm . As before, due to the lack of an explicit description of \mathcal{P}^\pm , the necessary algebra is performed over the corresponding \mathcal{T}^\pm . We represent the feasible set (3) in standard form through the addition of some slack variables for constraints (3b) and (3c). All feasible clusterings correspond to vertices of \mathcal{T}^\pm , and C_{rad}^s is optimal w.r.t. $c(s)$.

The desired transition in objective function over \mathcal{T}^\pm is $(1 - \lambda)c(s) + \lambda c(t)$ for increasing λ . This can equivalently be written in the form $c(s) + \lambda \Delta c$ for $\Delta c = c(t) - c(s)$ to fit the general formula. We are only interested in $\lambda > 0$, i.e., only upper bounds. When we hit the *breakpoint*

$$\left(\max_{j \in \mathcal{N}} -\frac{\Delta z_j}{z_j^*} \right)^{-1}, \tag{9}$$

we change the optimal basis. Generally, vertices of \mathcal{T}^\pm can be highly degenerate, so we might arrive at a (new) basis of the current vertex. An update of the underlying clustering happens when we take an actual step along an edge of \mathcal{T}^\pm to a new, adjacent vertex.

Algorithm 3: ALGORADTORAD($C_{\text{rad}}^s, C_{\text{rad}}^t, s, t, \kappa^-, \kappa^+$). Linear transition from radial clustering C_{rad}^s w.r.t. s to radial clustering C_{rad}^t w.r.t. t .

Input: Radial clusterings C_{rad}^s and C_{rad}^t w.r.t. site vectors $s \in \mathbb{R}^{d \cdot k}$ and $t \in \mathbb{R}^{d \cdot k}$;
cluster size bounds κ^\pm

Output: Sequence of radial clusterings and sequence of corresponding power diagrams that satisfy the properties of Theorem 3

```

1 Set  $\lambda, \lambda_0, r \leftarrow 0$  and  $C^{\lambda_0} = C_{\text{rad}}^s$ ;
2 while  $C^{\lambda_r} \neq C_{\text{rad}}^t$  do
3   Increase  $\lambda$  to the next ranging breakpoint such that  $c(s^\lambda) = \lambda c(t) + (1 - \lambda)c(s)$ 
   satisfies  $c(s^\lambda) \in N_{\mathcal{T}^\pm(\kappa^-, \kappa^+)}(C^{\lambda_r}) \cap N_{\mathcal{T}^\pm(\kappa^-, \kappa^+)}(C^\lambda)$  for some adjacent
   vertex/clustering  $C^\lambda \neq C^{\lambda_r}$ ;
4   Set  $r \leftarrow r + 1$ ,  $\lambda_r \leftarrow \lambda$  and  $C^{\lambda_r} \leftarrow C^\lambda$ ;
5   Compute a feasible solution for (8) with  $\bar{s} = s^{\lambda_r}$  and  $C^{\nu-1} = C^{\lambda_{r-1}}$ ,  $C^\nu = C^{\lambda_r}$ , and
   let  $\bar{P}^r$  be the corresponding power diagram;
6   if  $r \geq 2$  then
7     Solve LP (7) with  $\bar{s} = \frac{1}{2}(s^{\lambda_{r-1}} + s^{\lambda_r})$  and  $C^\nu = C^{\lambda_{r-1}}$  and let  $P^{\lambda_{r-1}}$  be the
     corresponding power diagram;
8   end
9 end
10 return sequence of clusterings  $(C^{\lambda_0}, C^{\lambda_1}, \dots, C^{\lambda_r})$ 
    and sequence of power diagrams  $(\bar{P}^{\lambda_1}, P^{\lambda_1}, \bar{P}^{\lambda_2}, \dots, P^{\lambda_{r-1}}, \bar{P}^{\lambda_r})$ 

```

We repeat this analysis iteratively, updating the dictionary for each new basis, to identify a sequence of breakpoints throughout the transition from $c(s)$ to $c(t)$. The result is a (simplified) parametric linear programming algorithm over \mathcal{T}^\pm . See ALGORADTORAD, Algorithm 3, for a description of the scheme in pseudocode. Figure 9 depicts an initial and target clustering, as well as an intermediate clustering in the linear transition. ALGORADTORAD is phrased in reference to the normal cones of consecutive vertices, which implies that changes in basis without leaving the current vertex are filtered out. Each clustering in the returned sequence is distinct from its predecessor. We perform an edge walk over \mathcal{T}^\pm . In Lemma 2 at the end of this section, we show that the corresponding clustering vectors are distinct, too, so that we obtain a proper walk along boundary points over \mathcal{P}^\pm , as well. Note that λ_r ($1 \leq r \leq m$) indicates the breakpoint where the objective vector $c((1 - \lambda_r)s + \lambda_r t)$ lies in the intersection of the normal cones of $C^{\lambda_{r-1}}$ and C^{λ_r} w.r.t. \mathcal{T}^\pm .

Compared to a general parametric linear program, we do not have to track and keep the parameter λ in the dictionary itself. The required algebra for \mathcal{T}^\pm , i.e., the update of the dictionary upon a basis change, is particularly simple because the underlying constraint matrix is totally-unimodular and has only entries 0 and 1. ALGORADTORAD also performs the computation of a sequence of power diagrams associated to the clusterings. Because of the linear change in sites throughout, there are some technical details that have to be addressed; see Section 3.2.

We prove correctness of ALGORADTORAD, along with a number of favorable properties of the

transition and output, in the following theorem.

Theorem 3. *Let C_{rad}^s and C_{rad}^t be radial clusterings w.r.t. site vectors s and t . Further, let κ^-, κ^+ be cluster size bounds such that $\kappa^- \leq |C_{rad}^s|, |C_{rad}^t| \leq \kappa^+$, and let $s^\lambda = (1-\lambda)s + \lambda t$. ALGORADTORAD returns a sequence of clusterings*

$$(C^{\lambda_0}, C^{\lambda_1}, \dots, C^{\lambda_r})$$

and a sequence of power diagrams

$$(\overline{P}^{\lambda_1}, P^{\lambda_1}, \overline{P}^{\lambda_2}, \dots, P^{\lambda_{r-1}}, \overline{P}^{\lambda_r})$$

that satisfy the following properties:

1. $C^{\lambda_0} = C_{rad}^s, C^{\lambda_r} = C_{rad}^t$
2. the C^{λ_i} are radial clusterings for sites $(1-\lambda_i)s + \lambda_i t$ for all $i \geq 0$
3. all clusterings have cluster sizes $|C_i|$ satisfying $\kappa_i^- \leq |C_i| \leq \kappa_i^+$ for all $i \leq k$
4. consecutive clusterings in the sequence differ by a single cyclical or sequential exchange of items
5. P^{λ_i} is a separating power diagram for C^{λ_i} for sites $\frac{1}{2}(s^{\lambda_{i-1}} + s^{\lambda_i})$
6. for each pair $C^{\lambda_{i-1}}, C^{\lambda_i}$ of consecutive clusterings, \overline{P}^{λ_i} is a shared power diagram for sites s^{λ_i}

Proof. Recall the informal description of ALGORADTORAD above. As before, most of the claimed properties are direct consequences of the design of the algorithm.

Line 1 is the initialization of the algorithm with $C^{\lambda_0} = C_{rad}^s$. C^{λ_r} for increasing r is the clustering that is worked on. Lines 3 – 7 are the steps in the main loop of the algorithm. They describe a step from the current clustering to a next one (lines 3 and 4), along with the computation of associated power diagrams (lines 5 to 8), until C^{λ_r} becomes equivalent to C_{rad}^t (line 2). The main idea is the creation of a sequence of clusterings $(C^{\lambda_0} = C_{rad}^s, C^{\lambda_1}, \dots, C^{\lambda_r} = C_{rad}^t)$ for increasing λ_i , where each clustering C^{λ_i} is a radial clustering for sites $s_i^\lambda = (1-\lambda_i)s + \lambda_i t$. Let us take a closer look at why such a sequence is created:

The algorithm keeps running as long as the current clustering is not C_{rad}^t (line 2). The number λ satisfies $\lambda = \lambda_{i-1}$ at the beginning of the i -th run of the while loop. In line 3, we increase λ until a ranging breakpoint (that satisfies an extra property) is hit. Recall that a breakpoint is a value of λ for which the current basis and a new basis are equally good w.r.t. the objective function $c(s^\lambda)$. For a highly degenerate vertex, multiple basis changes may have to be performed before a step to an adjacent vertex/clustering is performed. The wording of line 3 indicates that we continue to increase λ , respectively continue to perform basis changes, until we do so: $c(s^\lambda) = \lambda c(t) + (1-\lambda)c(s)$ now is optimal over $\mathcal{T}^\pm(\kappa^-, \kappa^+)$ for both the current clustering $C^{\lambda_{i-1}}$ and a new, next clustering C^λ . Both clusterings are radial for the sites s^λ over $\mathcal{P}^\pm(\kappa^-, \kappa^+)$. (In Lemma 2 below, we prove that the two clusterings have distinct clustering vectors, too - but this is not required for our arguments here.) The vectors $c(s^\lambda)$, respectively s^λ , are on the shared boundary of the normal cones for the clusterings in $\mathcal{T}^\pm(\kappa^-, \kappa^+)$, respectively $\mathcal{P}^\pm(\kappa^-, \kappa^+)$. The actual algebra to find a breakpoint is an evaluation of the term in Eq. (9) for the current clustering and $c = c(s_i^\lambda)$; the result gives $\lambda - \lambda_i$.

In the i -th iteration, line 4 is an increase of the iteration counter, the labeling of the breakpoint λ as λ_i , and the labeling of the new clustering C^λ as C^{λ_i} . Lines 5 to 8 describe the computation

of the associated power diagrams, which we turn to below. Then the next iteration of the loop is started. At the end of the algorithm, λ approaches 1. There exists a $\lambda_r \leq 1$ for which $C^{\lambda_r} = C_{\text{rad}}^t$, as $c(t) \in N_{\mathcal{T}^\pm}(C_{\text{rad}}^t)$ by construction, and the algorithm terminates. All computations are done over $\mathcal{T}^\pm(\kappa^-, \kappa^+)$, so all clusterings in the returned sequence have cluster sizes satisfying $\kappa_i^- \leq |C_i| \leq \kappa_i^+$ for all $i \leq k$. This proves properties 1, 2, and 3.

The sensitivity-analysis-based computation of a breakpoint and new, adjacent *vertex* (not only basis) of \mathcal{T}^\pm means that two consecutive clusterings are connected by a shared edge. Thus, they differ by a single cyclical or sequential exchange of items; see Proposition 3. This gives property 4. Overall, this proves that the algorithm terminates with a sequence of clusterings $(C^{\lambda_0}, C^{\lambda_1}, \dots, C^{\lambda_r})$ of the claimed properties.

It remains to prove properties 5 and 6, i.e., to prove that the constructed sequence of power diagrams $(\bar{P}^{\lambda_1}, P^{\lambda_1}, \bar{P}^{\lambda_2}, \dots, P^{\lambda_{r-1}}, \bar{P}^{\lambda_r})$ satisfies the claimed properties. Recall Section 3.2, where we described the LPs to find a separating power diagram for given sites and a given clustering, respectively a shared power diagram for given sites and a pair of clusterings. We have to show that our input allows for feasible solutions.

In the i -th iteration, the computation of a feasible solution for LP (8) in line 5 refers to the computation of a shared power diagram \bar{P}^{λ_i} for sites $\bar{s} = s^{\lambda_i}$ and the consecutive clusterings $C^\nu = C^{\lambda_i}$ and $C^{\nu-1} = C^{\lambda_{i-1}}$. The existence of a feasible solution, i.e., of a shared power diagram, follows from $c(s^{\lambda_i})$ being in the intersection of the normal cones $c(s^{\lambda_i}) \in N_{\mathcal{T}^\pm(\kappa^-, \kappa^+)}(C^{\lambda_{i-1}}) \cap N_{\mathcal{T}^\pm(\kappa^-, \kappa^+)}(C^{\lambda_i})$ (line 3). (Recall that $C^{\lambda_{i-1}}, C^{\lambda_i}$ correspond to adjacent vertices in \mathcal{T}^\pm .) Geometrically, any point on the edge between the vertices (and possibly a face of higher dimension) of $\mathcal{T}^\pm(\kappa^-, \kappa^+)$ contains $c(s^{\lambda_i})$ in its normal cone. Equivalently, there is a face of $\mathcal{P}^\pm(\kappa^-, \kappa^+)$ of at least dimension 1 with s^{λ_i} in its normal cone. Similar to the proof of Theorem 2, the fractional clusterings corresponding to points in this face allow for a separating power diagram that induces both $C^{\lambda_{i-1}}$ and C^{λ_i} – the desired shared power diagram \bar{P}^{λ_i} . This shows property 6.

Lines 6 to 8 describe the computation of a ‘good’ separating power diagram, maximizing the minimal margin, for all intermediate clusterings in the transition. The power diagram $P^{\lambda_{i-1}}$ is computed for $C^{\lambda_{i-1}}$ in the i -th iteration (for $i \geq 2$). It is performed through a solution of LP (7) for sites $\bar{s} = \frac{1}{2}(s^{\lambda_{i-1}} + s^{\lambda_i})$ and $C^\nu = C^{\lambda_{i-1}}$. Note that information on λ_i is required for the definition \bar{s} , which is why the computation of $P^{\lambda_{i-1}}$ for $C^{\lambda_{i-1}}$ appears at the end of the iteration that found the next C^{λ_i} .

The site vector \bar{s} lies on the line segment between the sites $s^{\lambda_{i-1}}$ at the breakpoints when transitioning to $C^{\lambda_{i-1}}$ and the sites s^{λ_i} when transitioning away from it, to C^{λ_i} . Thus, the vector \bar{s} lies in the normal cone of $w(C^{\lambda_{i-1}})$, respectively $c(\bar{s}) \in N_{\mathcal{T}^\pm(\kappa^-, \kappa^+)}(C^{\lambda_{i-1}})$. This implies that $C^{\lambda_{i-1}}$ allows for a separating power diagram for sites \bar{s} , and such a power diagram is found as a feasible solution to LP (7). This shows property 5.

Summing up, the returned sequence $(\bar{P}^{\lambda_1}, P^{\lambda_1}, \bar{P}^{\lambda_2}, \dots, P^{\lambda_{r-1}}, \bar{P}^{\lambda_r})$ is an alternating sequence of shared power diagrams and good power diagrams following the sequence of clustering and satisfying properties 5 and 6. This completes the proof. \square

We observed that, in an all-shape setting, i.e., when $\kappa^- = (0, \dots, 0)$ and $\kappa^+ = (n, \dots, n)$, the required algebra for basis updates and the breakpoint formula becomes especially simple. However, the special, simple form of radial clusterings in this setting, recall Figure 7, is a reason why we chose *not* to perform our walk over all-shape polytopes, to not impose such a special, possibly undesirable structure on the intermediate clusterings in the transition.

We conclude this section by showing that ALGORADTORAD, which is designed to construct a

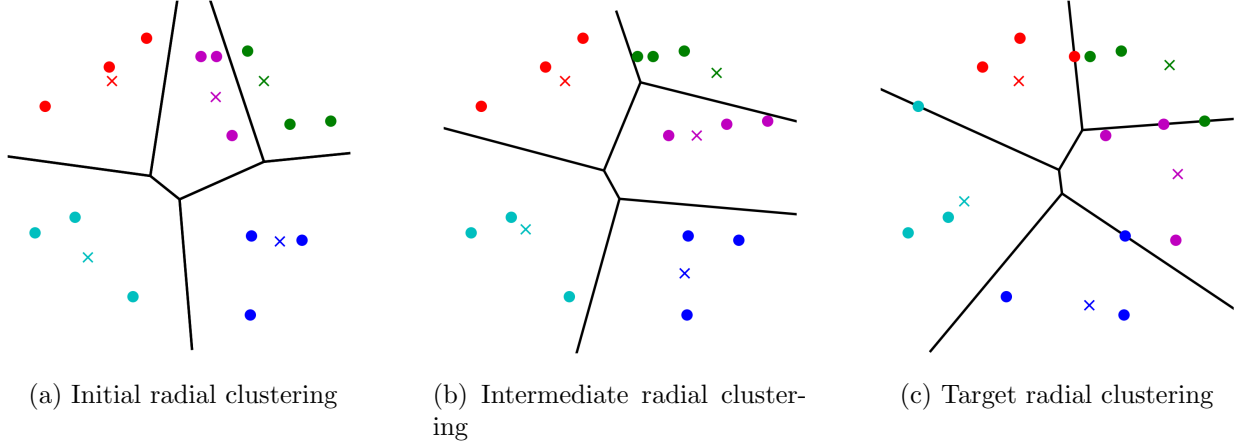


Figure 9: Initial, target, and one intermediate radial clustering in a linear transition as in ALGORADTORAD. The sites follow a linear transition from s , for the initial clustering, to t , for the target clustering. Note that the sites for the intermediate clustering lie on the line segment between their initial and target positions.

sequence of clusterings through an edge walk over a bounded-shape transportation polytope, also computes a (well-defined) walk along the boundary of the corresponding partition polytope. More specifically, we prove that consecutive clusterings in the returned sequence have distinct clustering vectors. Thus each step along an edge in the transportation polytope corresponds to a proper step along the boundary of the partition polytope. (Recall the discussion in Section 2.2 that highlights that one has to be careful in this transfer.)

Lemma 2. *Let $(C^{\lambda_0}, C^{\lambda_1}, \dots, C^{\lambda_r})$ be a sequence of clusterings returned by ALGORADTORAD. For every $1 \leq i \leq r$, $w(C^{\lambda_i}) \neq w(C^{\lambda_{i-1}})$.*

Proof. Line 3 of ALGORADTORAD ensures that $C^{\lambda_{i-1}} \neq C^{\lambda_i}$ for all $i \geq 1$. Further, the corresponding vertices $y^{\lambda_{i-1}}$ and y^{λ_i} of \mathcal{T}^\pm share an edge. By Proposition 3, the clustering difference graph $CDG(C^{\lambda_{i-1}}, C^{\lambda_i})$ contains a single cycle or path. For any fixed node $l \in [k]$ on this cycle or path, let x_l^+ and x_l^- be the label of the arc that enters, respectively leaves, node l in the CDG.

Since the items in data set $X \subset \mathbb{R}^d$ are distinct, i.e., we have $x_l^+ \neq x_l^-$. The component of the vector $w(C^{\lambda_i}) - w(C^{\lambda_{i-1}})$ corresponding to cluster l equals $\sum_{x \in C_l^{\lambda_i}} x - \sum_{x \in C_l^{\lambda_{i-1}}} x = x_l^+ - x_l^- \neq 0$, i.e., $w(C^{\lambda_i}) - w(C^{\lambda_{i-1}}) \neq 0$. Thus $w(C^{\lambda_i}) \neq w(C^{\lambda_{i-1}})$. \square

6 Conclusion

In this paper, we designed an algorithm to transition between two given constrained LSAs in the form of a sequence of clusterings that satisfies the many favorable properties listed in Theorem 1. We would like to highlight a few natural questions to study for further improvements.

First, a study and optimization of the efficiency of our methods would be of interest. As we use steps of the simplex method, and information from an optimal simplex tableau, current implementations have bottlenecks in the setup and solution of the underlying LPs. These are simple generalizations of classical transportation problems, and as such are well-understood. In addition

to a bound based on LP theory, it would be promising to study whether some of the LP-based steps of our algorithm (such as lines 3 and 4 in `ALGOINITTORAD` and line 3 in `ALGORADTORAD`) can be replaced by more efficient combinatorial algorithms.

Second, related to this is a desire for a bound on the number of steps of the transition. In particular, we are interested in providing a bound on the number of steps in the middle part of the transition, where radial clusterings are traversed. This part of the transition corresponds to an edge walk over \mathcal{T}^\pm , so that first bounds come from the combinatorial diameter or so-called circuit diameter of these polytopes; see [6, 10]. However, previous literature only takes into account the assignment of items to clusters, and not the locations of items in the underlying space. For the fixed-site transition from a general LSA to its radial counterpart, we do have a bound in the form of the number of feasible clustering shapes; see Theorem 2, property 7. Again, this bound does not take into account the locations of items in the space. In both cases, we believe better bounds can be derived through a use of this geometric information.

Finally, there are several ways that one can try to improve on the design of the current approach. We broke up the walk into three parts. Essentially, the walk from an initial LSA to its corresponding radial clustering (and from the target radial clustering to target LSA) serve as a pre-processing that allows the main part of the transition to be a walk between radial clusterings. In turn, this allowed the direct use of LP theory for the design of `ALGORADTORAD`. While the cluster sizes of initial and target clustering are typically very similar, and thus the use of radial clusterings in the transition not a noteworthy restriction (recall the discussion in Section 3), the first and final part of the transition do not change the sites. It would be interesting to study whether a similar walk can be computed without this hard three-part split, where a linear transition from the initial sites to the target sites happens throughout the whole walk. Such a transition could be more ‘direct’, in particular in view of the number of steps of the walk. There are many other ways that a ‘better’ transition could be designed - for example, a transition can be influenced by a translation of the data set itself, because the locations of items influence which LSAs are radial and not. One could impose additional restrictions of ‘monotone’ cluster sizes during the transition, i.e., cluster sizes may either only increase (if $|C_i^t| > |C_i^s|$) or only decrease (if $|C_i^t| < |C_i^s|$) - our algorithms in this paper only guarantee that we lie between the induced bounds. Further, in some applications it may be of interest to find a transition where in each step multiple exchanges of items, disjoint from each other so that they can be applied in parallel, are desired. For all of these possible improvements, we expect the design of a (combinatorial) algorithm to be challenging, because it will not suffice to use the well-understood relationship between LSAs (and power diagrams) and linear programming over partition and transportation polytopes.

Acknowledgements. Borgwardt gratefully acknowledges support of this work through NSF award 2006183 *Circuit Walks in Optimization*, Algorithmic Foundations, CCF, Division of Computing and Communication Foundations, and through Simons Collaboration Grant 524210 *Polyhedral Theory in Data Analytics* before. Happach has been supported by the Alexander von Humboldt Foundation with funds from the German Federal Ministry of Education and Research (BMBF).

References

- [1] F. Aurenhammer. Power diagrams: Properties, algorithms and applications. *SIAM Journal on Computing*, 16(1):78–96, 1987.

- [2] F. Aurenhammer, F. Hoffmann, and B. Aronov. Minkowski-type theorems and least-squares clustering. *Algorithmica*, 20(1):61–76, 1998.
- [3] E. R. Barnes, A. J. Hoffman, and U. G. Rothblum. Optimal partitions having disjoint convex and conic hulls. *Mathematical Programming*, 54(1-3):69–86, 1992.
- [4] K. P. Bennett and O. L. Mangasarian. Multicategory discrimination via linear programming. *Optimization Methods and Software*, 3:27–39, 1992.
- [5] S. Borgwardt. *A Combinatorial Optimization Approach to Constrained Clustering*. PhD thesis, Technische Universität München, 2010.
- [6] S. Borgwardt. On the diameter of partition polytopes and vertex-disjoint cycle cover. *Mathematical Programming*, 141(1-2):1–20, 2013.
- [7] S. Borgwardt. On soft power diagrams. *Journal of Mathematical Modelling and Algorithms in Operations Research*, 14(2):173–196, 2015.
- [8] S. Borgwardt and F. Happach. Good clusterings have large volume. *Operations Research*, 67(1):215–231, 2019.
- [9] S. Borgwardt and C. Viss. Circuit walks in integral polyhedra. *Discrete Optimization*, in press, 2020.
- [10] S. Borgwardt and C. Viss. Constructing Clustering Transformations. *SIAM Journal on Discrete Mathematics*, in press, 2020.
- [11] E. J. Bredensteiner and K. P. Bennett. Multicategory classification by support vector machines. *Computational Optimization and Applications*, 12:53–79, 1999.
- [12] A. Brieden and P. Gritzmann. On optimal weighted balanced clusterings: Gravity bodies and power diagrams. *SIAM Journal on Discrete Mathematics*, 26(2):415–434, 2012.
- [13] K. Crammer and Y. Singer. On the algorithmic implementation of multiclass kernel-based vector machines. *Journal on Machine Learning Research*, 2:265–292, 2002.
- [14] K. Fukuda, S. Onn, and V. Rosta. An adaptive algorithm for vector partitioning. *Journal of Global Optimization*, 25(3):305–319, 2003.
- [15] F. K. Hwang, S. Onn, and U. G. Rothblum. Representations and characterizations of vertices of bounded-shape partition polytopes. *Linear Algebra and its Applications*, 278(1-3):263–284, 1998.
- [16] B. Schölkopf and A. Smola. *Learning with Kernels*. MIT Press, 2002.
- [17] R. J. Vanderbei. *Linear Programming*. Springer, 2016.
- [18] V. Vapnik. *Statistical learning theory*. Wiley, 1998.
- [19] J. Weston and C. Watkins. Support vector machines for multi-class pattern recognition. In *Proceedings of the Seventh European Symposium On Artificial Neural Networks (ESANN)*, pages 219–224, 1999.